Effect of capsule shape on hydrodynamic characteristics and optimal design of hydraulic capsule pipelines.

ASIM, T., ALGADI, A. and MISHRA, R.

2018

Effect of Capsule Shape on Hydrodynamic Characteristics and Optimal Design of Hydraulic Capsule Pipelines

Taimoor Asim[*1], Abdualmagid Algadi[2] and Rakesh Mishra[3]
[1,2,3] School of Computing & Engineering
University of Huddersfield, Queensgate, Huddersfield HD1 3DH, UK
[1]t.asim@hud.ac.uk, [2]Abdualmagid.Algadi@hud.ac.uk, [3]r.mishra@hud.ac.uk

Abstract
Hydraulic capsule pipelines (HCPs) are the third generation pipelines transporting hollow containers, known as capsules. These capsules are filled with material/cargo to be transported. The shape of these capsules has a significant effect on the hydrodynamic flow characteristics within HCPs. As the variations in the pressure distribution within HCPs are directly linked to and the flow characteristics within pipelines, it is essential to critically evaluate the effect of capsule shape on the pressure drop across the pipeline. Published literature is severely limited in terms of establishing the effects of the shape of the capsules on the flow characteristics within pipelines. Hence, the present study focuses on using a well-validated Computational Fluid Dynamics tool to numerically simulate the flow of capsules of various shapes quantified in form of a novel shape factor in hydraulic capsule pipelines. Both on-shore and off-shore applications of such pipelines have been investigated in the present study, along-with pipe fittings, such as bends. Variations in flow related parameters within these pipelines have been discussed in detail for a wide range of geometrical parameters associated with the capsules and the pipelines. Pressure drop values have been used to develop novel semi-empirical prediction models as a function of the shape factor and other flow and geometric variables of the capsules. These prediction models have been embedded into a pipeline optimisation methodology, which has been developed based on Least-Cost Principle. The resulting novel optimisation methodology can be used for hydraulic capsule pipeline design. Performance charts for practical applications have been developed for easy implementation of the design methodology for the designers of hydraulic capsule pipelines transporting capsule of different shapes.

Keywords: Hydraulic Capsule Pipeline (HCP), Least-Cost Principle, Optimisation, Shape Factor, Solid-Liquid Flow

1.0 Introduction
Capsule transportation through pipelines is an established mode of bulk solid handing, which is extensively employed in a number of industries i.e. mining industry, process industry, chemical industry etc. In many applications capsules that are being transported do not have any preferential shape. This makes estimation of flow characteristics within transportation pipelines difficult, which in turn affects poor design of such pipelines. Currently the effect of variations in capsule shape is accounted for by defining a shape factor as per the equation given below.

$$\psi = \left(\frac{\text{Volume of Capsule}}{\text{Volume of Circumscribing Sphere}}\right)^{\frac{1}{3}} \quad (1)$$

Ellis et al [1-5] carried out a number of experimental investigations on the flow of both equi-density and heavy-density capsules of shape factors of 1 (spherical) and 0.8094 (cylindrical,

[*] Corresponding Author
Tel.: +44 1484 472323

with length equal to capsule's diameter, as defined in equation (1)), where equi-density and heavy-density refers to the capsules having the same and higher densities than their carrier fluid respectively. The size of the capsules varied from k=0.39 to k=0.89, where k=d/D, d and D being the diameters of the capsules and the pipeline respectively. The flow conditions investigated ranged from average flow velocity (V_{av}) of 1 m/s to 3.7 m/sec. Capsules' velocities (V_c) have been recorded in all these experiments. It has been reported that the capsule velocity is dependent on a range of different geometrical and flow related parameters, such as shape factor of the capsule, k, V_{av}, length of the capsules (L_c), specific gravity of the capsules (s), spacing between the capsules (S_c) etc. For example, it has been reported that as the shape factor decreases, holdup (which is capsule to water velocity ratio i.e. $H=\frac{V_c}{V_{av}}$) increases. Similarly, capsules of smaller diameters propagate faster in the pipeline as compared to the capsules of larger diameters. Due to the nature of these studies being experimental, only limited information could be obtained regarding local flow characteristic in the vicinity of the capsules. Moreover, as the optimisation of HCPs includes information related to the pressure drop within such pipelines, these studies could not be used for such purposes. Experimental investigations similar to Ellis et al have been carried out by Kruyer et al [6] concluding that the capsule velocity decreases as its diameter decreases. Latto et al [7] and Hwang et al [8] have concluded that the length of the capsules has little effect on the efficiency of the system, while Tachibana [9] stated that capsules of lower shape factors offered less energy loss with HCPs. Tsuji et al [10] concluded that the presence of multiple capsules affected the flow structure within HCPs, while Ohashi et al [11] concluded that the pressure drop within HCPs was inversely proportional to the Froud Number. The same conclusions have been drawn by Bartosik et al [12] and Yanaida et al [13] as well.

Chow's [14] experimental investigations are perhaps amongst the first where the effects of a range of different geometrical and flow related parameters were enumerated on both the capsule velocity and the pressure drop within HCPs. However, the primary limitation of Chow's analysis is that it is being carried out for off-shore applications (vertical pipelines) only. As the flow structure within horizontal and vertical HCPs is quite different (because heavy-density capsules in horizontal pipes propagate along the bottom wall of the pipe, whereas, they travel along the centre-line in case of vertical pipes), Chow's results cannot be used for on-shore applications of HCPs. Mathur et al [15], Agarwal et al [16] and Mishra et al [17-18] conducted experimental investigations on the flow of capsules of shape factor (ψ) of 1 in HCPs, focusing on developing relationships for capsules' velocity.

Ulusarslan et al [19-27] have carried out extensive experimental instigations on the transport of capsules of ψ=1 in HCPs for on-shore applications (i.e. horizontal pipelines), developing expressions for capsules' velocity and pressure drop within the HCP. It has been reported that increase in the average flow velocity has negligible effect on the spacing between the capsules. Moreover, it has been reported that as the size of the capsule increases, the pressure drop across the pipeline increases. It has also been reported that the pressure drop across pipe bends is significantly higher as compared to equivalent straight pipe length. Vlasak et al [28-29] conducted experimental studies on the flow of heavy-density capsules of ψ=0.8094 in HCP bends. It has been reported that as the shape factor of the capsules decreases, the hydraulic gradient across the pipeline increases. The capsule velocity has been considered to be equal to the average flow velocity in these investigations, which is a major limitation of the work. It has been observed that as the average flow velocity increases, capsule velocity also increases. However, no information regarding the local flow structure within the pipe bends has been reported.

The majority of works that have been reported on HCPs involve transportation of capsules of ψ=1 and 0.8094. Kyuyer et al [30] presented an analytical analysis on the flow of heavy-density capsules of ψ=0.8094 in the laminar flow of water; however, Charles [31] and Kroonenberg [32] conducted theoretical studies on the turbulent flow of equi-density and heavy-density capsules of ψ=1.5 in HCPs respectively. Both Charles and Kroonenberg have developed analytical expressions for capsules' velocity and the pressure drop (ΔP) within HCPs. While Charles assumed that both V_c and ΔP being functions of k only, Kroonenberg neglected actual velocity profiles within the different sections of the HCP (such as the annulus region between the capsule and the pipeline), considering only mean velocities. These assumptions make these studies more theoretical than practical, as Round et al's [33] experimental investigations conclude that V_c is function of both k and V_{av}. In these works, the effect of capsule's shape factor has not been explored.

Newton et al [34] conducted perhaps the first numerical investigation on the flow of a capsule of ψ=0.8094-0.3838 (cylindrical with varying lengths) in an HCP. The range of investigations is the same as considered by Ellis et al [1-5]; however, the flow is considered to be laminar in the study; same as Kyuyer et al [30]. Tomita et al [35-36] carried out numerical investigations on both a single and a train of capsules in HCPs, where capsule/s have been considered as point masses, assuming a fully developed co-axial flow in the annulus between the capsule and the pipe wall. Capsules' velocity and trajectory have been reported in detail. Lenau et al [37] extended Tomita et al's work by considering a single capsule as both elastic and rigid body respectively, however, no discussions on the shape factor or the pressure drop within HCPs is presented in these studies. Khalil et al [38-39] carried out numerical investigations on the flow of a capsule of ψ=0.3838 (long cylinder) in HCPs. A comparison of various turbulence models has been presented. Velocity profiles and pressure drop calculations have been analysed in detail. However, the shape factor of the capsule has been taken to be the same for all the cases in the investigation. A limited analysis of the flow field within the pipeline has been presented.

All the above works significantly enhance the understanding of capsule flow in pipelines, resulting in development of HCP's design principles, however, these studies are severely limited in systematically analysing the effect of the shape of the capsule on the hydrodynamic behaviour and the optimal design of HCPs. Most of these studies provide information on flow around regular shaped capsules, however, most capsules may be slightly asymmetric, and hence new investigations are needed for complex shaped capsules. With regards to the optimal design of HCPs, Polderman [40] reports design rules for both on-shore and off-shore applications of HCPs. The design rules are based on the pressure drop in the pipeline, Reynolds number etc. A general indication towards parameters that might be used for an optimisation model has been provided. However, no optimisation model has been developed, which can be used to design an HCP for practical applications. Assadollahbaik et al [41] developed an optimisation model for pipelines transporting capsules, based on maximum pumping efficiency. The costs involved in the design of such pipelines are, however, not included. Swamee [42] has developed an optimisation model for sediment transport pipelines based on the least-cost principle. The model assumes the value of the friction factor as the input to the model, strictly limiting its usefulness for commercial applications. Swamee [43] has further developed a model for the optimisation of equi-density capsules of φ=0.8094, in a hydraulic pipeline, based on least-cost principle. The friction factors considered, however, are not representative of the capsule flow in the pipeline, and hence severely limit the practicality of the model.

Agarwal et al [44] has developed an optimisation model for multi-stage pipelines transporting capsules. The model is based on least-cost principle and uses the solid throughput as input to the model. The model developed is applicable for contacting capsules only, occupying the complete length of the pipeline. Furthermore, a homogeneous model for pressure drop prediction has been considered, where the friction factor used for the model is an approximation of the Colebrook-White's equation [45], severely limiting the utility of the model in terms of accurate representation of the pressure drop in the pipeline transporting capsules. Sha et al [46] also developed an optimisation model for hydraulic pipelines based on saving energy sources. The model, however, cannot be used for multi-phase flows.

Asim et al [47-50] have carried out detailed numerical investigations on the flow of both equi-density and heavy-density capsules of ψ=1 to 0.3838 for both on-shore and off-shore applications, including pipe bends. A wide range of geometrical and flow related parameters have been considered. Prediction models for the pressure drop in HCPs have been developed. HCP design optimisation methodology has been developed, based on least-cost principle. The pressure drop prediction models have been integrated with the optimisation model for practical design purposes. However, the primary concern with these studies is that the different capsule shapes have been treated separately. Furthermore, separate prediction models have been developed of both equi-density and heavy-density capsules. Hence, there is an exhaustive list of prediction models from which the HCP designers have to choose the most appropriate ones for precise modelling of HCPs.

The present study is an improvement in Asim et al's [47-50] works where, the effect of shape of capsules with unequal mass distribution, in addition to the three most common shapes of the capsules (i.e. spherical, cylindrical and rectangular), have been represented in a single set of design equations. Variations in the orientation of the capsules with end nose have also been analysed in the present study. For commercial viability of HCPs, it is quite evident that these pipelines need to be designed optimally for widespread acceptability for wide ranging capsules. The designers are in need of a design methodology which accounts for the hydraulic and mechanical design of a pipeline transporting capsules. Hence, an optimisation model has been developed, which is both robust and user-friendly. The optimisation model is based on the fact that the total cost involved in the design of a pipeline transporting capsules is minimum.

2.0 Hydrodynamic analysis of HCPs

Darcy's equation for the pressure drop in a pipeline can be extended to compute pressure drop within HCPs carrying capsules of different specific gravities and sizes by separating the pressure drop within the pipeline due to water alone, and due to capsules only [51].

$$\Delta P_m = k_1 f_w \frac{L_p}{D} \frac{k_2 \rho_w (1-c) k_3 V_{av}^2}{2} + k_4 f_c \frac{L_p}{D} \frac{k_5 \rho_w c k_6 V_{av}^2}{2} \quad (2)$$

where ΔP_m represents the pressure drop across the pipe due to the mixture flow, ρ_w is the density of water, c is the concentration of the solid phase in the mixture, V_{av} is the average flow velocity and the constants k_1, k_2, k_3, k_4, k_5, k_6 are the coefficients which relate the friction factor, density and the velocity of both the water and the capsules respectively to that of the mixture. Representing the effects of the concentration of the solid phase (c) and the constants k_1, k_2, k_3, k_4, k_5, k_6 in terms of friction factor due to water alone (f_w) and friction factor due to capsules only (f_c), equation (2) can be simplified as:

$$\Delta P_m = f_w \frac{L_p}{D} \frac{\rho_w V_{av}^2}{2} + f_c \frac{L_p}{D} \frac{\rho_w V_{av}^2}{2} \quad (3)$$

Equation (3) is valid for the horizontal HCPs. This equation can be extended further to include the elevation effects as:

$$\Delta P_m = f_w \frac{L_p}{D} \frac{\rho_w V_{av}^2}{2} + f_c \frac{L_p}{D} \frac{\rho_w V_{av}^2}{2} + \rho_w g \Delta h_w \quad (4)$$

where g is the gravitational acceleration and Δh_w is the elevation of the water column. Hence, equations (3) and (4) represent the major loses in both on-shore and off-shore HCPs.

In order to compute the minor loses within HCPs, the following expressions for the loss coefficients of bends have been derived:

$$\Delta P_m = K_{lw} \frac{n \rho_w V_{av}^2}{2} + K_{lc} \frac{n \rho_w V_{av}^2}{2} \quad (5)$$

$$\Delta P_m = K_{lw} \frac{n \rho_w V_{av}^2}{2} + K_{lc} \frac{n \rho_w V_{av}^2}{2} + \rho_w g \Delta h_w \quad (6)$$

where K_{lw} represent the loss coefficient of the bend due to water, K_{lc} is the loss coefficient of the bend due to capsule and n is the number of bends attached to the pipeline. Friction factors and loss coefficients in equations (3-6) can be determined using well verified numerical methods, which can also provide useful information regarding the flow structure within HCPs.

3.0 Numerical modelling of HCPs

The numerical model of the hydraulic capsule pipeline considered in the present study has three sections i.e. an inlet pipe, a test section and an outlet pipe, where the lengths of these three sections are 5 m, 1 m and 1 m respectively, as shown in figure 1(a). A 5 m long inlet pipe is used in order to allow the flow to become fully developed [52]. A 1m long outlet pipe has been used to minimise the effects of the outlet boundary condition in the test section of the pipeline. The test section is similar to that of [19-27, 47-50] with a 100 mm internal diameter. The pipe surface has been considered to be hydrodynamically smooth, with an absolute roughness constant (ε) of zero. Five different shaped capsules, as shown in figure 1(b), have been numerically analysed in the present study. The pressure drop data for the basic capsule shapes i.e. spherical, cylindrical and rectangular capsules have already been published by the authors [47-50]. The new shapes include cylindrical capsules with hemispherical and conical ends. These end shapes are expected to improve the hydrodynamic behaviour of the capsules. Moreover, in order to cover a wide range of geometrical variations within pipelines, vertical pipelines and two pipe bends of r/R=4 and 8 have also been considered for analysis in the present study [53].

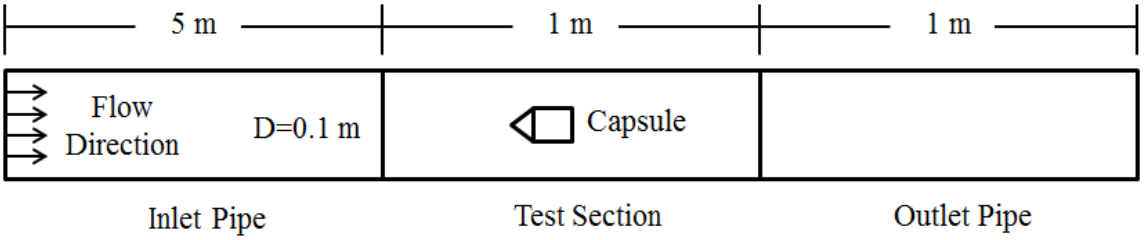

(a)

(b)

Figure 1 (a) Numerical model of the HCP (b) Capsule shapes considered

As three basic capsule shapes (i.e. spherical, cylindrical and rectangular), and two complicated shapes (i.e. hemispherical and conical ends) have been considered in the presented study, a shape factor (φ) has been defined to reflect the variations in the shapes of the capsules. The shape factor considered in the present study has been defined as a ratio of the surface area of the capsule to the mid-plane cross sectional area of an equivalent sphere (i.e. having same volume as the capsule). An additional term, based on the distance of the centre of gravity from the upstream end of the capsule, has also been included to accurately reflect the orientation of the complicated shapes of the capsules. The mathematical representation of the shape factor considered in the present study is:

$$\varphi = \frac{SA_c}{2\ CSA_{equi-sphere}} - \frac{Vo_1 L_1 + Vo_2 L_2}{(Vo_1 + Vo_2)\ \bar{L}} \quad (7)$$

where SA_c is the surface area of the capsule and $CSA_{equi\text{-}sphere}$ is the mid-plane cross sectional area of a sphere having the same volume as the capsule. Vo_1 and Vo_2 are the upstream side and downstream side volumes of the capsule, as shown in figure 2. L_1 and L_2 are the distances from the upstream end of the capsule, to their respective centre of gravities (i.e. CGs), while $\bar{L}$ is the length of upstream section of the capsule. The first term on the right hand side of equation (7) takes into account the effect of the shape of the capsule/s, while the second term accounts for the orientation of the capsule/s. In case of regular shaped capsules (i.e. spherical, cylindrical and rectangular), the second term in equation (7) is equal to 1.

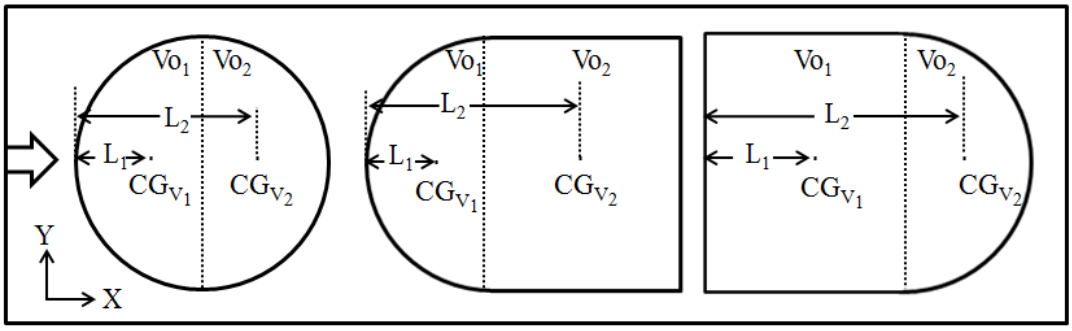

Figure 2 Representation of the shape factors of the capsules

Table 1 summarises the variations in the shape factor for the shapes considered in the present study. It can be seen that the shape factor of the spherical capsules is 1. The shape factor increases as the capsule's sphericity decreases. Hence, for a cylindrical capsule of length equal to its diameter (i.e. L_c=1d), the shape factor is 2.289, which is 129 % higher than the spherical capsule. Furthermore, as the shape of the capsule changes to rectangular, the shape factor further increases to 2.481 (for L_c=1d). It is however interesting to note that when a cylindrical capsule is attached with an end nose, its shape factor decreases, because of its increased sphericity. This decrease in the shape factor is dependent on the shape of the end

nose. Hence, a hemispherical end reduces the shape factor of a cylindrical capsule (for L_c=1d) by 127 %, whereas a conical end reduces it by 124 %. It can be further seen that as the orientation of the capsule changes (for example, the end nose is towards the downstream side of the capsule), the shape factor increases. This effect is discussed in detail later.

Table 1 Shape factors for different shaped capsules

Capsule shape	L_c	φ
Spherical	N/A	1
Cylindrical with Hemispherical end	1d	1.004
Cylindrical with Conical end	1d	1.020
Cylindrical with Reversed cylindrical end	1d	1.304
Cylindrical with Reversed conical end	1d	1.395
Cylindrical	1d	2.289
	3d	2.568
	5d	2.871
Rectangular	1d	2.481
	3d	2.784
	5d	3.112

The test section of the HCP has been spatially discretised into an unstructured mesh of tetrahedral elements, while both the inlet and outlet pipes contain structured hexehedral elements. The combined element count of the flow domain is approximately 1 million. The concentration and the level of refinement of the mesh elements within the test section in general, and in the vicinity of the capsule/s in particular, have a substantial impact on the accuracy of CFD predictions. Hence, the mesh quality has been controlled in a manner that, in the vicinity of the capsule/s, the flow domain consists of smaller mesh elements to capture the complex flow phenomena accurately and consequently to provide reliable results. This methodology allows an effective discretisation of the flow domain that leads to much more efficient use of computational resources.

In order to ensure that the numerical simulations are not influenced by the meshing controls, a mesh independence study has been carried out. The mesh has been refined/coarsened by dividing the flow domain into more/less number of mesh elements (element count of 0.5, 0.75, 2, 3 and 4 million). The independence of the simulation from the mesh density has been judged by the variation of the mixture pressure drop values across the test section of the HCP, for all the meshes considered. Table 2 shows the values of the mixture pressure drop across the test section for all the meshes. By examining the results, it is evident that the mixture pressure drop does not vary significantly beyond 1 million elements in the flow domain, and hence this mesh has been chosen for further analysis in the present study.

The inlet boundary of the flow domain has been modelled as a velocity inlet, where the inlet flow velocity can vary from 1 to 4 m/sec, depending on the operating conditions considered, as considered by many other researchers [19-27, 47-50]. The outlet boundary of the flow domain has been modelled as a pressure outlet at atmospheric conditions. Both the pipe and

the capsule walls have been modelled as hydrodynamically smooth walls, where the pipe wall is kept stationary, while the capsule walls translate with capsule velocity (V_c) [54-56].

Table 2 Mesh independence results

Number of mesh elements	Pressure at Inlet (Pa)	Pressure at outlet (Pa)	Mixture pressure drop per unit length (Pa/m)
0.5 million	9498	-25	9523
0.75 million	10269	225	10044
1 million	11163	401	10762
2 million	11265	584	10681
3 million	11230	509	10721
4 million	11204	471	10733

The capsules' velocities have been reported in detail by Asim et al [47-50], however, there are separate expressions for the different shapes of the capsules. Based on the definition of the shape factor in equation (7), and the velocity data from Asim et al, new holdup (capsule to average flow velocity ratio) expressions have been developed for on-shore applications:

Table 3 Boundary conditions

Boundary name	Boundary type	Boundary conditions
Inlet to the pipe	Velocity inlet	1–4 m/sec
Outlet of the pipe	Pressure outlet	0 Pa(g)
Wall of the pipe	Stationary wall	No-Slip
Capsules	Moving walls	From Literature/experiments

$$\frac{V_c}{V_{av}} = \frac{1.2\,(\varphi+1)^{0.041}}{(s+1)^{0.203}\,k^{0.053}\left(\frac{kD}{L_c}+1\right)^{0.006}} \tag{8}$$

and off-shore applications:

$$\frac{V_c}{V_{av}} = \frac{2.8\,k^{0.031}}{(\varphi+1)^{0.053}\,(s+1)^{0.97}\left(\frac{kD}{L_c}+1\right)^{0.286}} \tag{9}$$

where the Reynolds number (Re) of the capsule/s is defined as:

$$Re_c = \frac{\rho_c V_c d}{\mu} \tag{10}$$

Equations (8-9) are valid over a wide range of Reynolds number (100,000 – 400,000) in a 4inch pipeline with a circular cross-section, with capsules of k from 0.5 to 0.9, L_c from 1d to 5d and specific gravities from 1 to 2.7. In order to check the validity of these equations, holdup values from these equations have been compared against holdup values given by Asim et al [47-50]. Comparison of holdup values is shown in figure 3 for both on-shore and

off-shore applications. It can be seen that more than 95 % of the data points lie within ± 10% error band in case of horizontal HCPs, and within ±15 % error band in case of vertical HCPs.

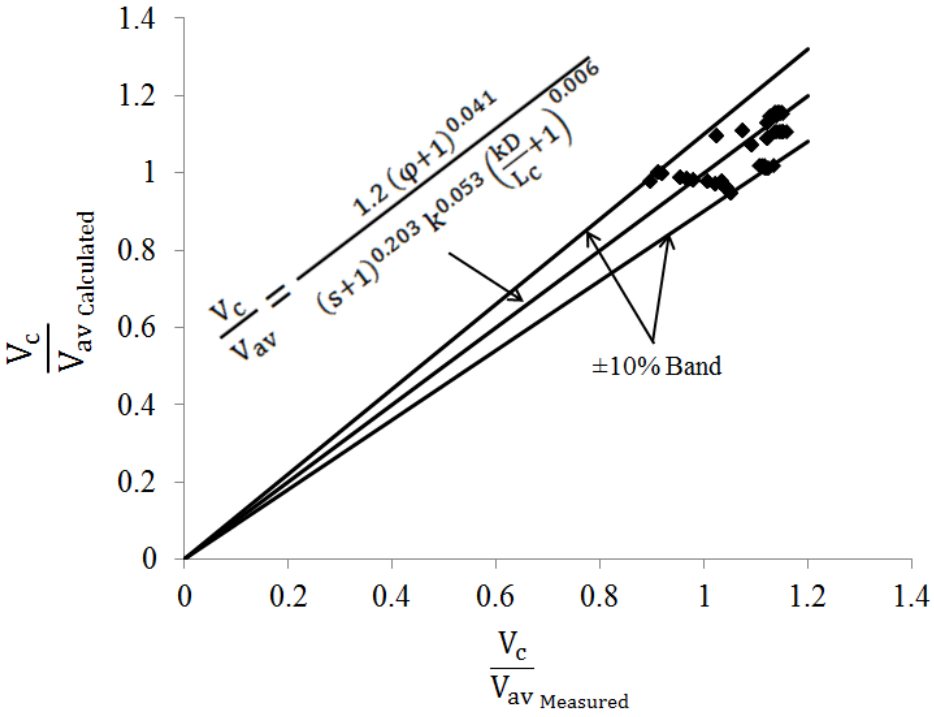

(a)

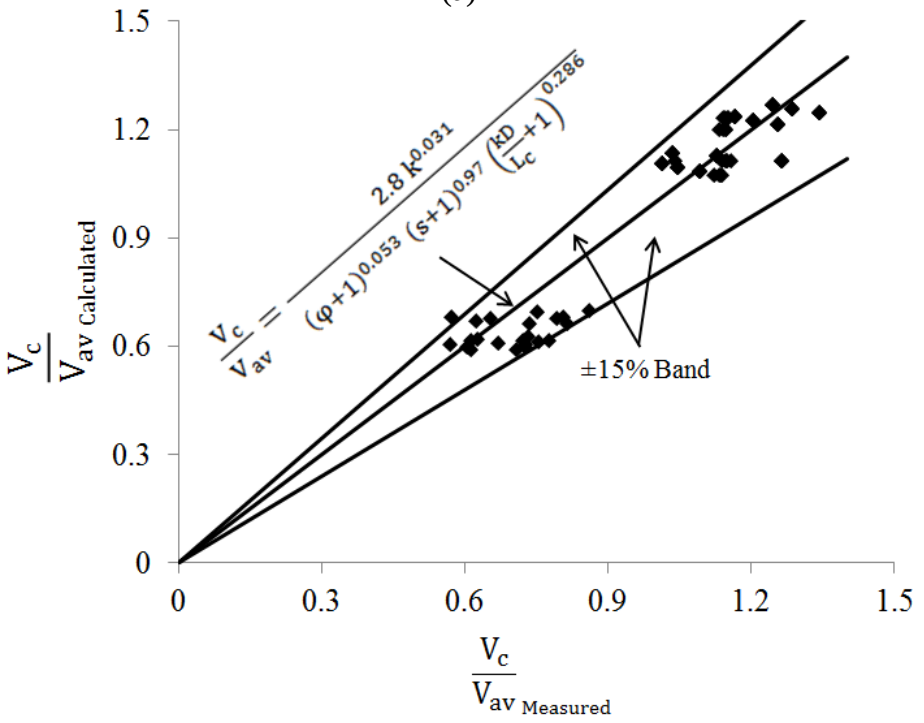

(b)

Figure 3 Comparison between calculated and measured holdup values for (a) horizontal pipes (b) vertical pipes

Three dimensional Navier-Stokes equations, alongwith the mass conservation equation, have been numerically solved, using Finite Volume Method, in an iterative manner, for the turbulent flow of water in HCPs. Shear Stress Transport (SST) k-ω turbulence model has been used to model the turbulence within the flow domain. Both the density and the viscosity

of water have been assumed constant (i.e. 998.2 kg/m^3 and 0.001003 Pa-sec respectively), while normal atmospheric pressure has been prescribed as the operating condition. Second order discretisation schemes for pressure, momentum and the turbulence parameters have been used for higher accuracy. In order to verify the CFD predicted results, experimental investigations have also been carried out. The details of the experimental setup are presented in the next section.

4.0 Hydraulic capsule pipeline setup

A 2inch diameter flow loop has been constructed to determine the capsule velocities under varying operating conditions. The experimental investigations have been limited to horizontal HCPs only. The pipework in the development of the flow loop are made of impact resistant unplasticised polyvinyl chloride (PVC). The maximum operating pressure that pipes and fittings can bear is 16 bar. A 1 m x 1 m x 1 m water tank has been connected to a Wilo CronoLine-IL 100/210-37/2 centrifugal pump by a PN16 flange (according to EN 1092-2). The maximum delivery pressure of the centrifugal pump is 16 bar, while the maximum pumping fluid temperature is 120 ºC. The rated power of pump's motor is 37 kW at 2900 rpm, while the motor efficiency ranges from 92 % to 93.7 %. The average flow velocity (V_{av}) has been controlled by changing the pump's flow rate. An 11 kW Siemens Optima Pump test rig has been used to control the flow rate of water passing through the pump. A digital turbine flow meter has been used to the HCP for monitoring the flow rate passing through the pipeline. The turbine flow meter used has an accuracy of ±3 % and a pressure rating of 225 psi at 22.7 ºF, while it can measure flow rates up to 760 ltrs/min. The capsule injection mechanism, as shown in figure 4, consists of a number of valves to restrict water flow in it while injecting the capsules into the system. A 1.75 m long horizontal pipe section serves as the test section for recording the capsule velocity.

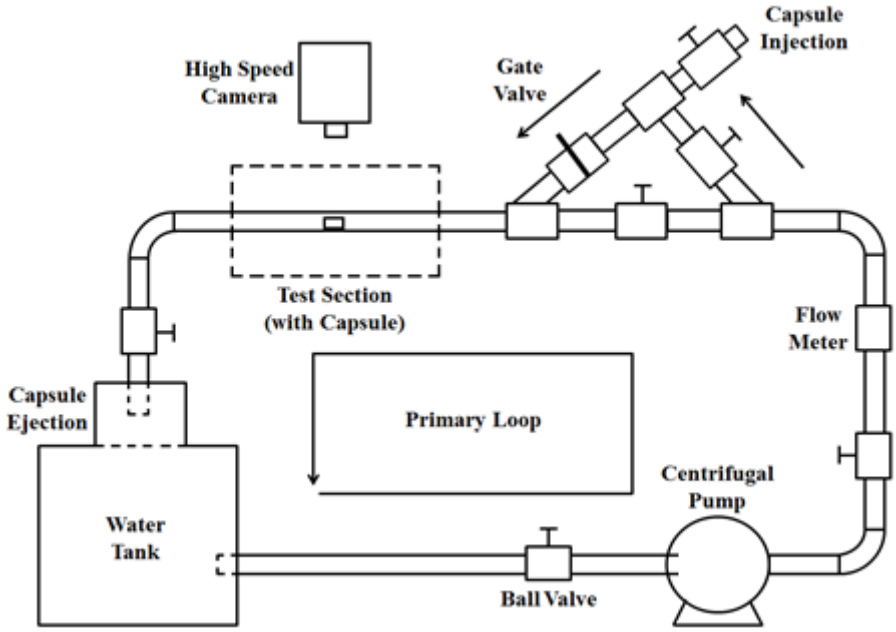

Figure 4 Schematic of the hydraulic capsule pipeline setup

A Photron FASTCAM SA3 high speed camera is mounted perpendicularly to the test section to capture images of the flowing capsule/s at a frame rate of 1000 fps, with an image resolution of 1024x512. The camera has been connected to the monitoring station via a 1000BASE-T Gigabit Ethernet Interface and a LAN cable with specifications beyond CAT5e standard. The capsule is collected on the top of the water tank by a metallic sieve, while the

water is drained into the tank. Figure 5 depicts two instances where a heavy-density capsule of φ=1 and capsule-to-pipe diameter ratio (k) of 0.7 is being transported by water at an average flow velocity (V_{av}) of 2.32 m/sec within the test section. It can be seen that as the capsule is heavy-density, it propagates along the bottom wall of the pipe.

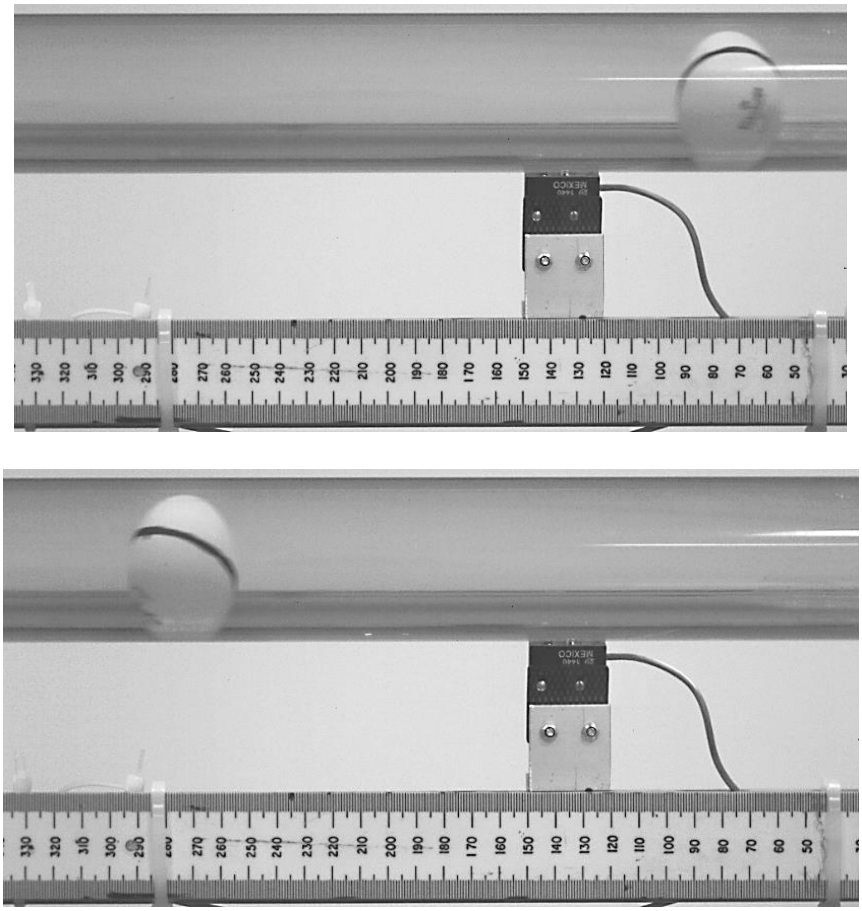

Figure 5 Flow path of a heavy-density capsule of φ=1 and k=0.7 at V_{av}=2.32 m/sec at two different instances

Table 4 summarises the experimentally recorded heavy-density capsule velocity data for φ=1, k=0.5 and 0.7. Comparison between equation (8) and the experimental findings has also been shown. It can be clearly seen that both the results are in close agreement, at different V_{av} and k values, and hence equation (8) has been used to find out capsule's velocities at other operating conditions in horizontal HCPs.

Table 4 Capsule velocity comparison

k	V_{av} (m/sec)	V_c from equation (8) (m/sec)	V_c from experiments (m/sec)	Difference in V_c (%)
0.5	2.18	1.99	2.03	2.01
	3.06	2.79	2.70	3.23
	3.20	2.92	2.85	2.40
0.7	2.18	2.12	2.08	1.89
	3.06	2.97	3.06	3.03
	3.20	3.11	3.19	2.57

Further verification of the pressure drop in HCPs has been carried out by comparing CFD findings with the experimental findings of Ulusarslan [19], as shown in table 5. Mixture pressure drop across the test section has been recorded at different average flow velocities. It can be seen that the CFD predicted pressure drop values are in close agreement with the experimentally recorded pressure drop values, at different operating conditions. Average variation of less than 5 % at all solid phase concentrations (c) has been recorded. It can thus be concluded that the numerical model considered in the present study represents the physical model of a pipeline, transporting capsules, accurately.

Table 5 Comparison of experimental and CFD predicted mixture pressure drops at different solid-phase concentration within a horizontal HCP

Re	ΔP_m experimental (in Pa) at different solid phase concentrations			ΔP_m CFD (in Pa) at different solid phase concentrations		
	5%	10%	15%	5%	10%	15%
20000	35	45	50	35	45	50
40000	90	100	110	88	98	105
60000	220	230		205	225	
80000	375	380		379	395	
90000	510			508		

5.0 Effect of shape factor on the flow field within HCPs

As discussed earlier, the complex flow phenomena associated with the transport of capsules in hydraulic pipelines has not been extensively reported in the published literature. There is a need to understand the hydrodynamic behaviour of the capsules of different shapes within an HPC to quantify the capsule shape effects on the pressure drop across the pipeline. This has been carried out in the present study, with a focus on explicitly establishing relationships between the shape of the capsules and the local flow parameters, like pressure coefficient, velocity etc., and hence on the global performance parameters, like pressure drop etc. The pressure coefficient definition used in the present study is:

$$P_c = \frac{P - P_{atm}}{0.5\rho V_{av}{}^2} \tag{11}$$

where P is the local static gauge pressure and P_{atm} is the atmospheric pressure. The CFD predicted pressure drop values have been used to develop novel semi-empirical expressions for the pressure drop within HCPs, which in-turn has been embedded into the HCP optimisation methodology developed for the flow of capsules of various shape factors in HCPs.

5.1 Horizontal HCPs

Figures 6 and 7 depict the local variations in the pressure coefficient and the flow velocity magnitude within the test section of the horizontal pipe respectively, transporting equi-density capsules of capsule-to-pipe diameter ratio of 0.5 at an average flow velocity of 1 m/sec. The length of the cylindrical and rectangular capsule considered here is equal to the hydraulic diameter of the capsules, hence φ=2.289 and 2.481 respectively. The inlet of the test section is on the left, hence, the flow direction is from left to right. It can be seen in

figure 6 that the presence of a capsule makes the pressure distribution highly non-uniform within the HCP, as compared to single phase flow where it is known that static pressure remains constant along the radial direction at a particular pipe cross-section [57]. The pressure gradients are fairly large upstream the capsule. The higher upstream pressure coefficient is due to the difference between the average flow velocity and the capsule velocity. This is associated with reduction in the flow velocity upstream the capsule, as depicted in figure 7.

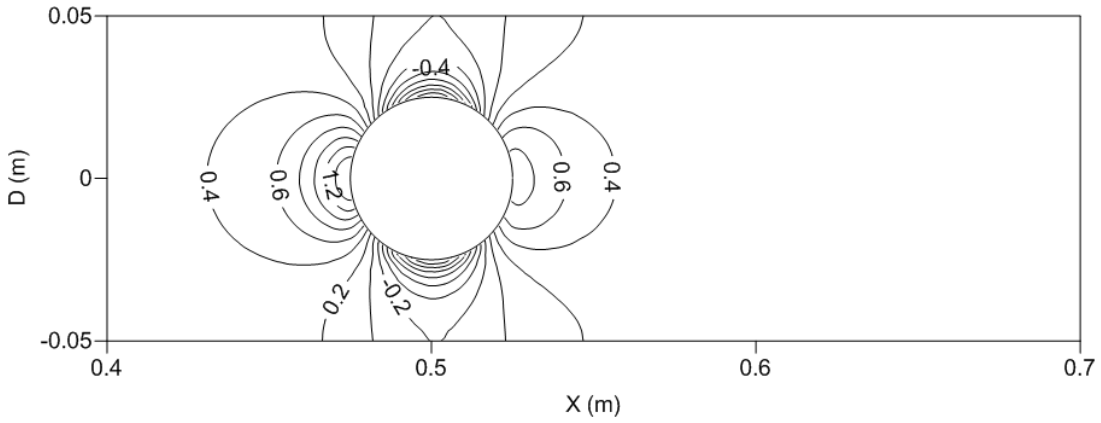

(a)

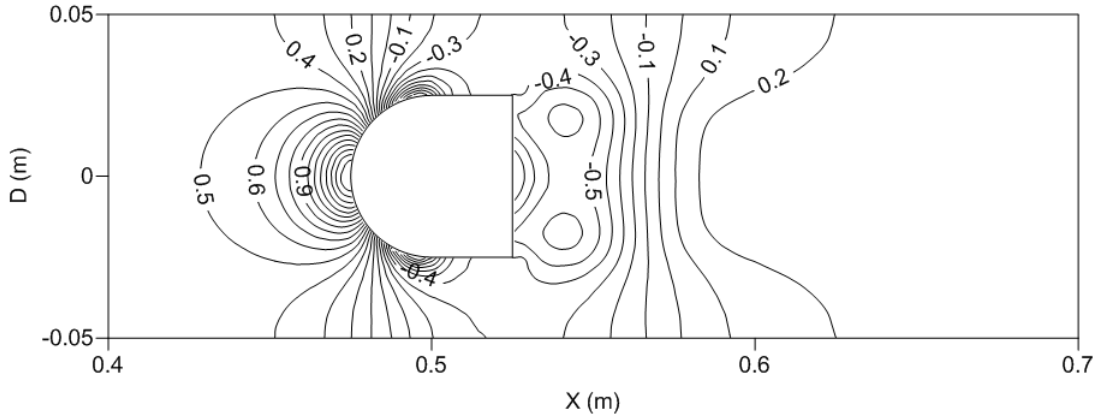

(b)

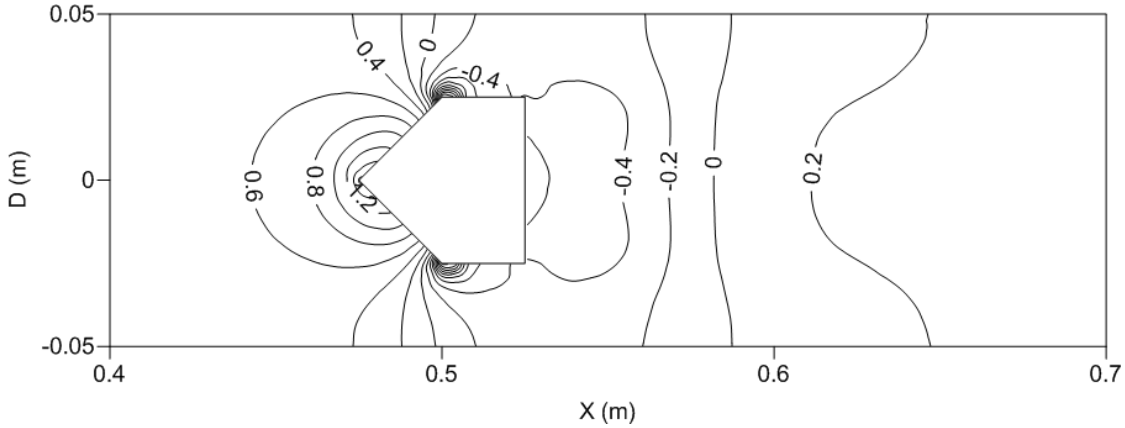

(c)

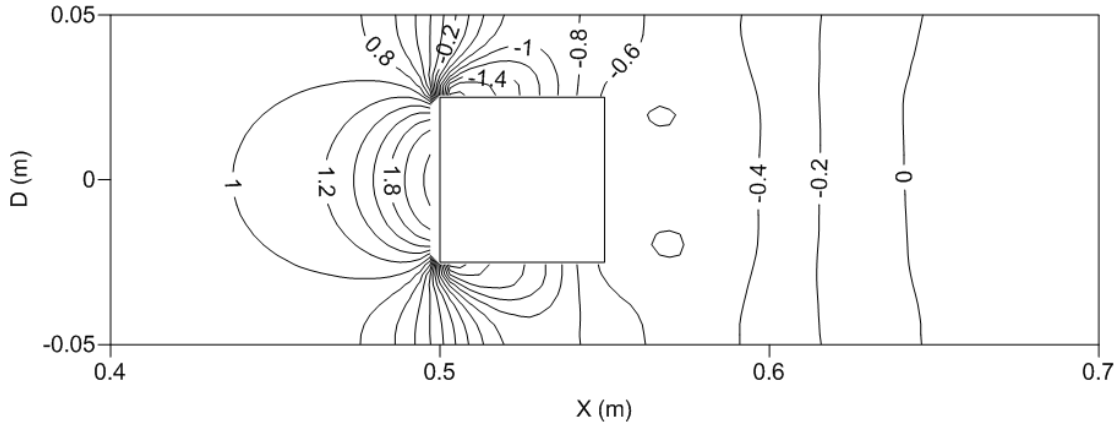

(d)

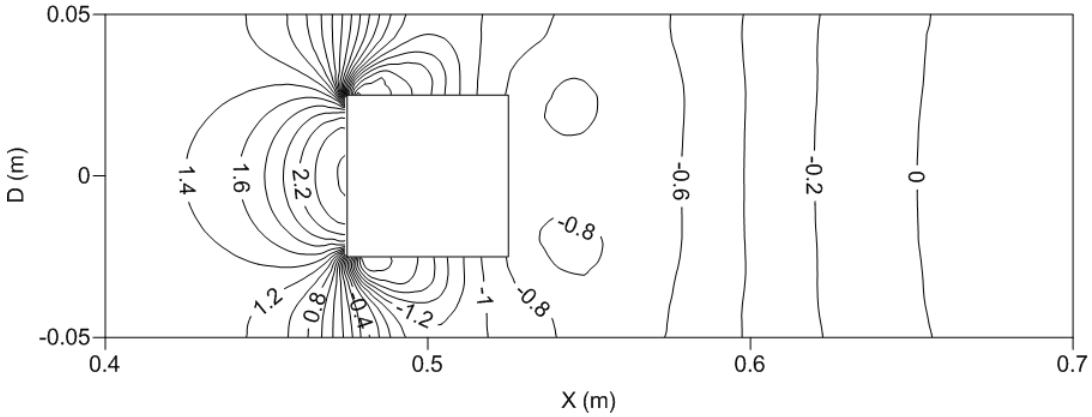

(e)

Figure 6 Pressure coefficient variations within a horizontal HCP for the flow of a single equi-density capsule of (a) φ=1 (b) φ=1.004 (c) φ=1.02 (d) φ=2.289 (e) φ=2.481 of k=0.5 at V_{av}=1 m/sec

The flow enters the annulus region between the pipe wall and the capsule. As the cross-sectional area decreases, the flow accelerates, resulting in reduction in the static pressure. The flow, while exiting the annulus region, decelerates, resulting in increase in the pressure coefficient. Downstream the capsule, the pressure coefficient recovers to some extent while the wake region of the capsule extends further downstream. Comparing the flow fields associated with different shaped capsules, it can be seen that the pressure coefficient distribution upstream the capsules remain fairly the same for all the different shape factors. However, there is a significant difference in the upstream static pressure coefficient values, which are higher for flat shaped (φ=2.289 and 2.481) capsules. Flow separation has been observed to occur on peripheral edges of the front face in these shapes. Furthermore, vortical structures have been noticed to emerge from the rear periphery of the capsules with sharp edges (except for φ=1). The pressure drops across the test section for φ=1, 1.004, 1.02, 2.289 and 2.481 are 147 Pa, 174 Pa, 211 Pa, 319 Pa and 414 Pa respectively, where the contributions of the capsules alone are 55 Pa, 82 Pa, 119 Pa, 227 Pa and 322 Pa respectively. Hence, it can be concluded that as the shape factor of the capsule increases, the pressure drop across the HCP also increases.

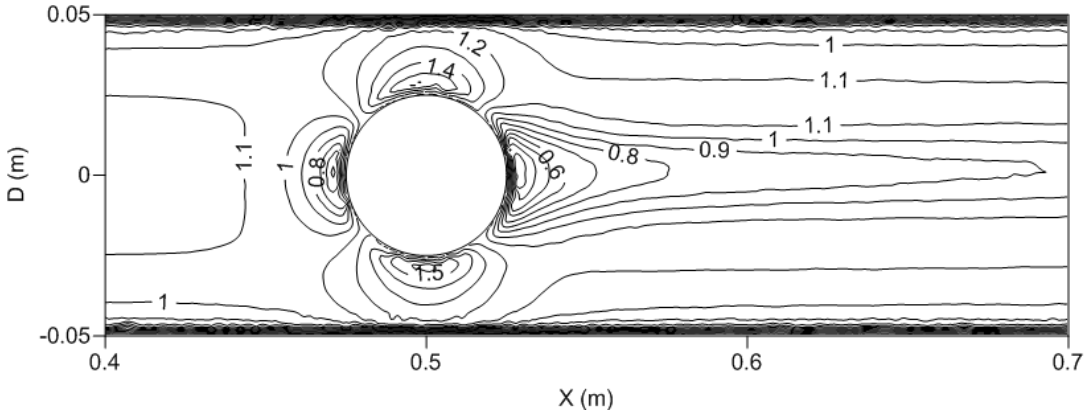
0.05
0
-0.05
D (m)
0.4
0.5
0.6
0.7
X (m)
1.2
1.4
1
1.1
1.1
1.1
0.8
0.9
1
0.6
0.8
1.5
1
1

(a)

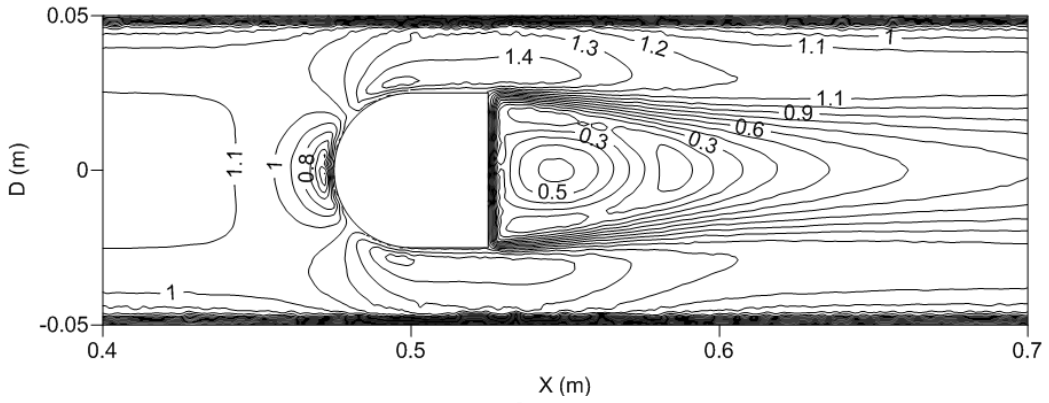
0.05
0
-0.05
D (m)
0.4
0.5
0.6
0.7
X (m)
1.4
1.3
1.2
1.1
1
1.1
0.9
0.6
0.3
0.3
0.5
1.1
0.8
1
1

(b)

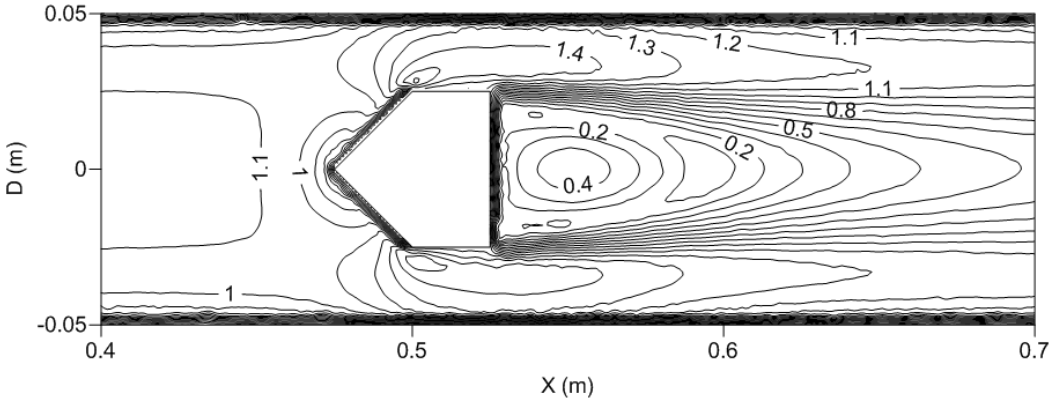
0.05
0
-0.05
D (m)
0.4
0.5
0.6
0.7
X (m)
1.4
1.3
1.2
1.1
1.1
0.8
0.5
0.2
0.2
0.4
1.1
1
1

(c)

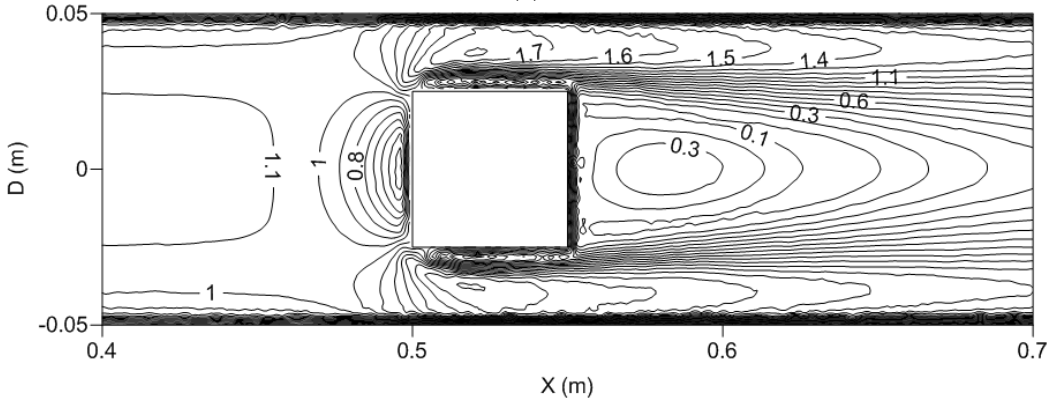
0.05
0
-0.05
D (m)
0.4
0.5
0.6
0.7
X (m)
1.7
1.6
1.5
1.4
1.1
0.6
0.3
0.1
0.3
1.1
0.8
1
1

(d)

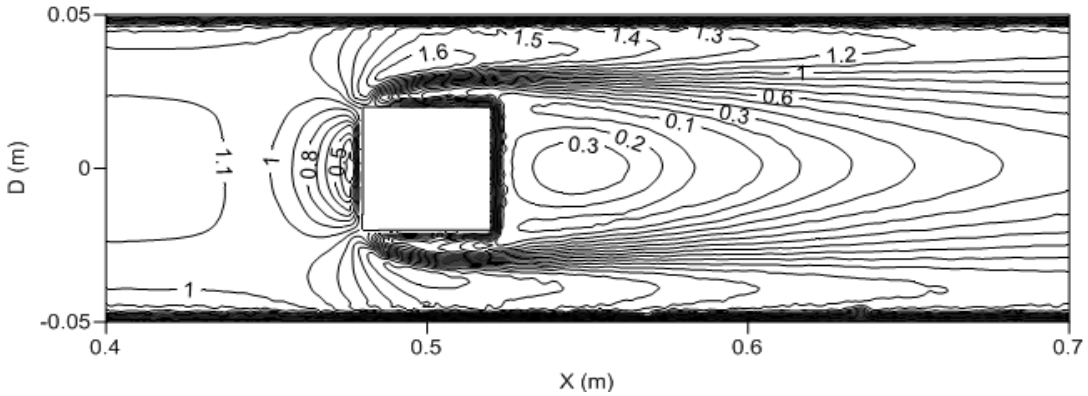

(e)

Figure 7 Flow velocity magnitude variations (in m/sec) within a horizontal HCP for the flow of a single equi-density capsule (a) φ=1 (b) φ=1.004 (c) φ=1.02 (d) φ=2.289 (e) φ=2.481 of k=0.5 at V_{av}=1 m/sec

5.2 Vertical HCPs

Figures 8 and 9 depict the local variations in the pressure coefficient and the flow velocity magnitude within the test section of the horizontal pipe respectively, transporting equi-density capsules of capsule-to-pipe diameter ratio of 0.5 at an average flow velocity of 1 m/sec. The inlet of the test section is on the bottom, hence, the flow direction is from bottom to top. The general trends observed are similar to the one observed in case of horizontal HCPs. It can be seen in figure that the presence of capsules makes the pressure coefficient distribution non-uniform within the HCP, however, as compared to horizontal HCPs, these non-uniformities are restricted to a much shorter distance both upstream and downstream the capsules. The pressure drops across the test section for φ=1, 1.004, 1.02, 2.289 and 2.481 are 9953 Pa, 9991 Pa, 10028 Pa, 10132 Pa and 10231 Pa respectively, out of which the contribution of the elevation is 9898 Pa. Hence, the actual contribution of the capsules of φ=1, 1.004, 1.02, 2.289 and 2.481 towards the pressure drop is 55 Pa, 93 Pa, 130 Pa, 234 Pa and 333 Pa respectively. In comparison with the horizontal HCPs, it can be clearly seen that the contribution of the capsules towards the pressure drop within both horizontal and vertical HCPs is the same. The difference in the capsules' pressure drop contributions is due to capsules' shape factor only. It can thus be concluded that as the shape factor increases, the pressure drop within an HCP increases.

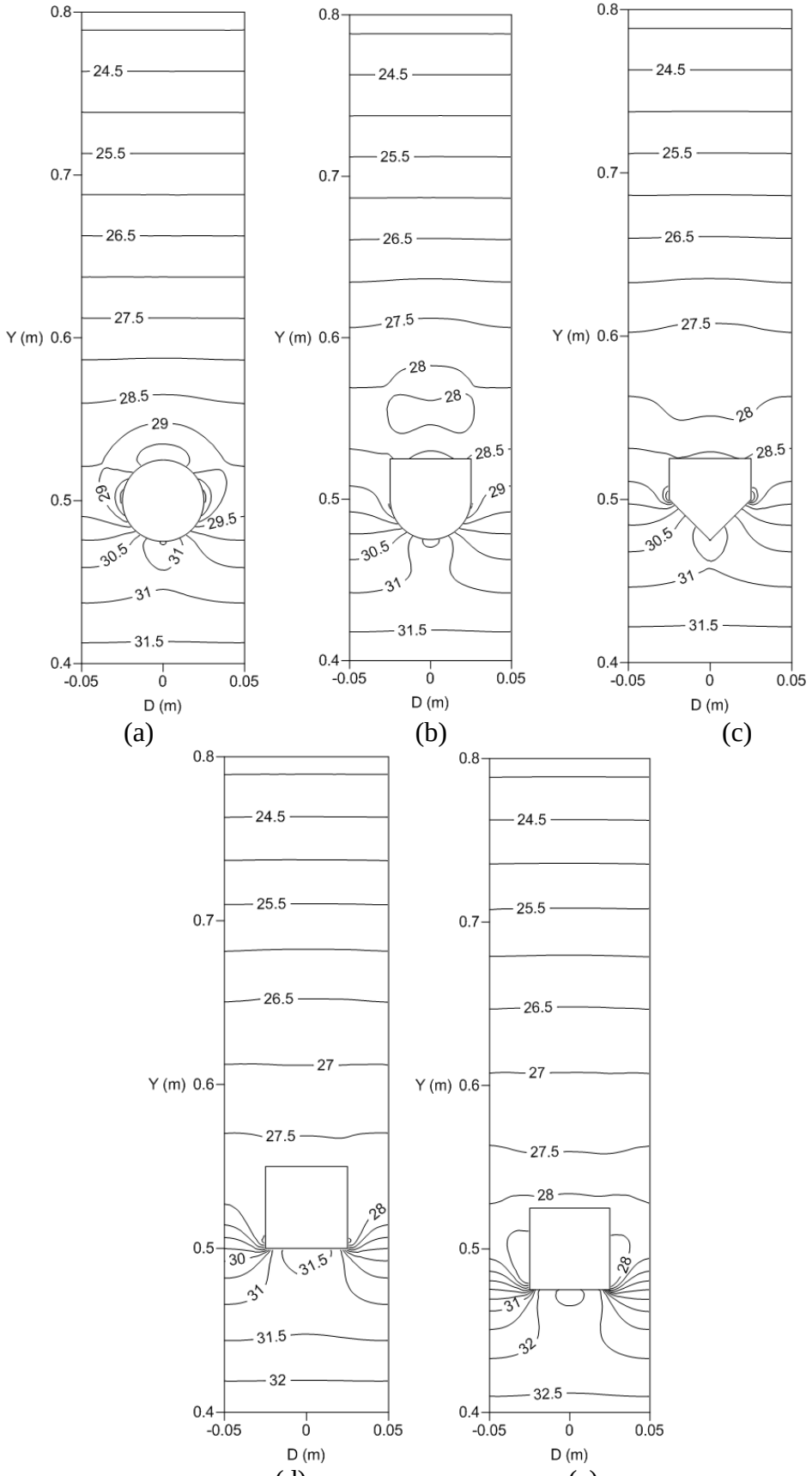

Figure 8 Pressure coefficient variations within a vertical HCP for the flow of a single equi-density capsule of (a) φ=1 (b) φ=1.004 (c) φ=1.02 (d) φ=2.289 (e) φ=2.481 of k=0.5 at V_{av}=1 m/sec

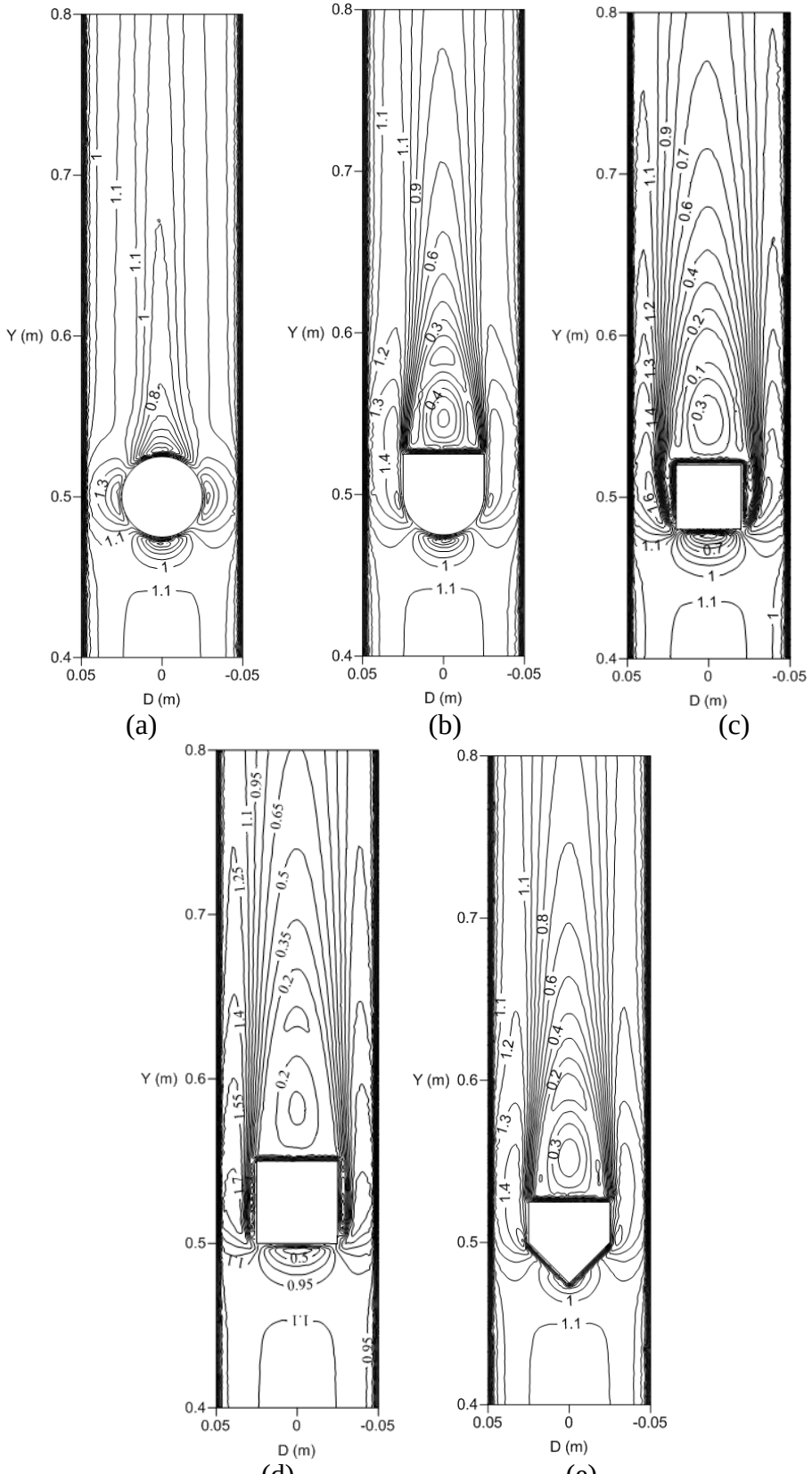

Figure 9 Flow velocity magnitude variations (in m/sec) within a vertical HCP for the flow of a single equi-density capsule of (a) φ=1 (b) φ=1.004 (c) φ=1.02 (d) φ=2.289 (e) φ=2.481 of k=0.5 at V_{av}=1 m/sec

5.3 HCP Bends

Figures 10 and 11 depict the local variations in the pressure coefficient and the flow velocity magnitude within an HCP bend of r/R=4 respectively, transporting equi-density capsules of capsule-to-pipe diameter ratio of 0.5 at an average flow velocity of 1 m/sec. It can be seen that both the pressure and the velocity fields are highly non-uniform, and are strongly dependent on the position and orientation of the capsules within the bend. Although the pressure distribution is somewhat similar upstream the capsule, it is very different downstream it for different capsules. The secondary flow generating capability within an HCP bend is considerably more as compared to straight HCP pipes. The pressure drops across the test section for φ=1, 1.004, 1.02, 2.289 and 2.481 are 169 Pa, 201 Pa, 262 Pa, 305 Pa and 522 Pa respectively. Hence, it can be seen that the pressure drop in HCP bends is higher than in HCP pipes, and it increases as the shape factor of the capsules increases.

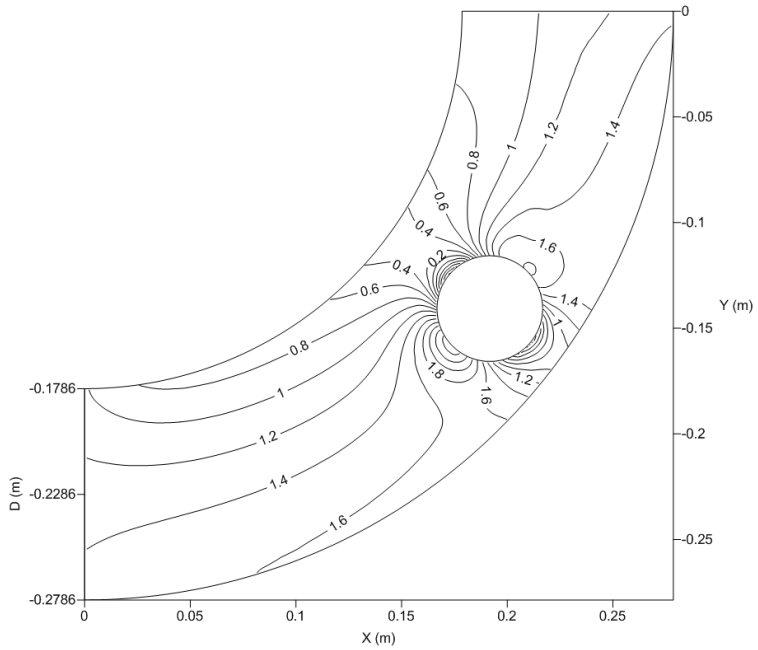

(a)

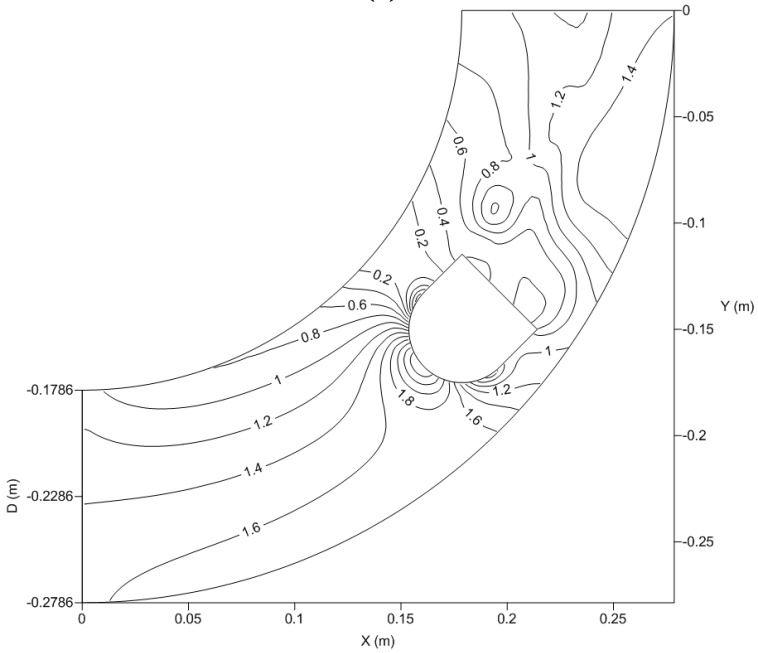

(b)

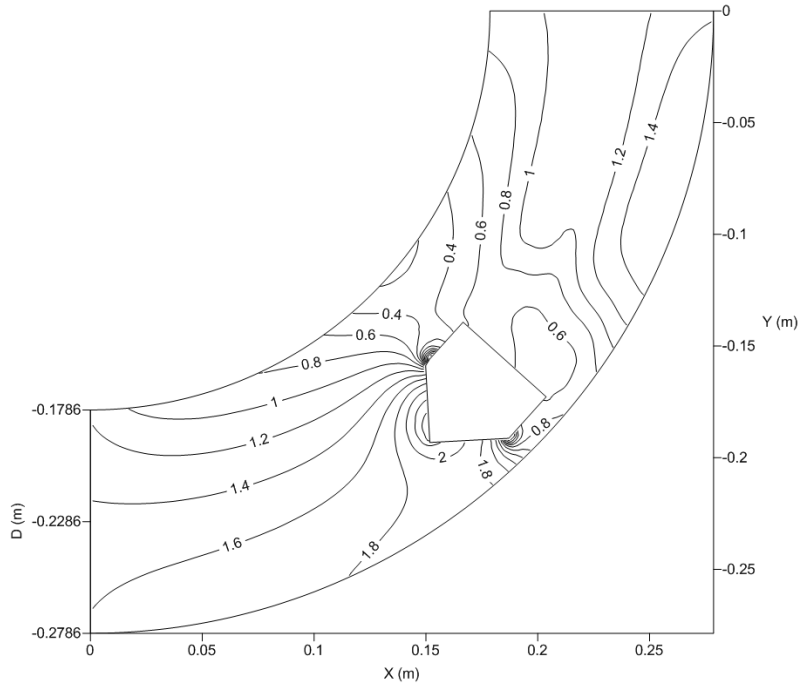
0
-0.05
-0.1
-0.15
-0.2
-0.25
Y (m)
-0.1786
-0.2286
-0.2786
D (m)
0
0.05
0.1
0.15
0.2
0.25
X (m)
0.4
0.6
0.8
1
1.2
1.4
1.6
1.8
2

(c)

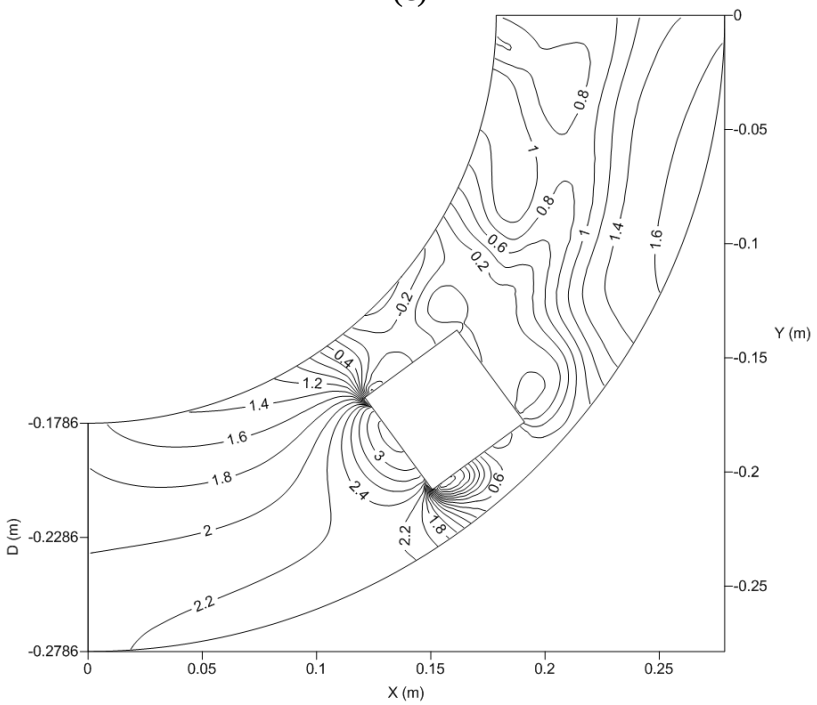
0
-0.05
-0.1
-0.15
-0.2
-0.25
Y (m)
-0.1786
-0.2286
-0.2786
D (m)
0
0.05
0.1
0.15
0.2
0.25
X (m)
0.2
0.4
0.6
0.8
1
1.2
1.4
1.6
1.8
2
2.2
2.4
3

(d)

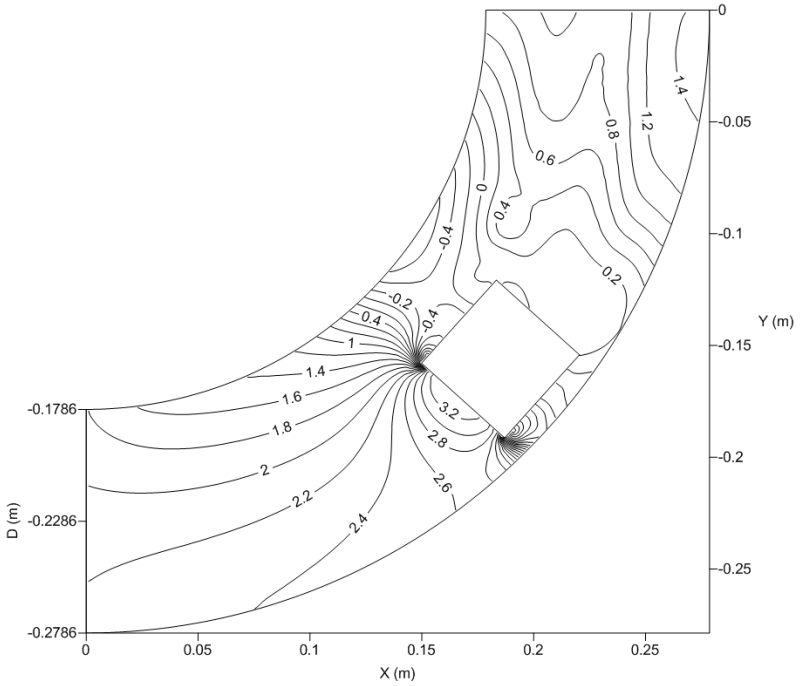

(e)

Figure 10 Pressure coefficient within a horizontal HCP bend for the flow of a single equi-density capsule of (a) φ=1 (b) φ=1.004 (c) φ=1.02 (d) φ=2.289 (e) φ=2.481 of k=0.5 at V_{av}=1 m/sec

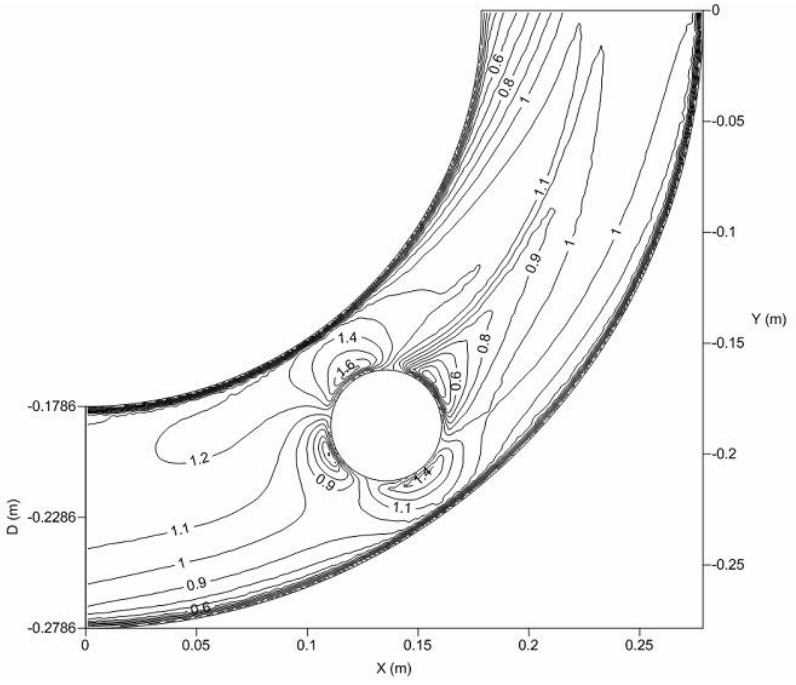

(a)

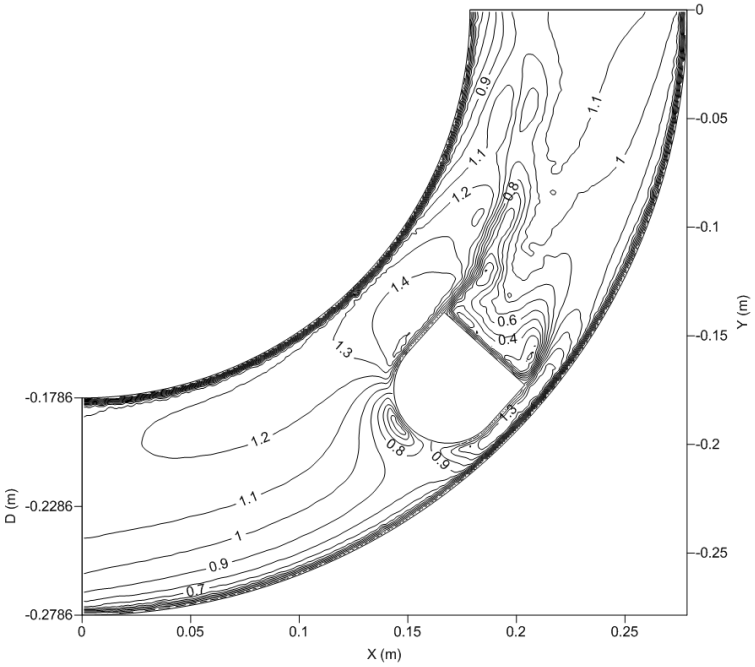
D (m)
X (m)
Y (m)
-0.1786
-0.2286
-0.2786
0
0.05
0.1
0.15
0.2
0.25
-0.05
-0.1
-0.15
-0.2
-0.25

(b)

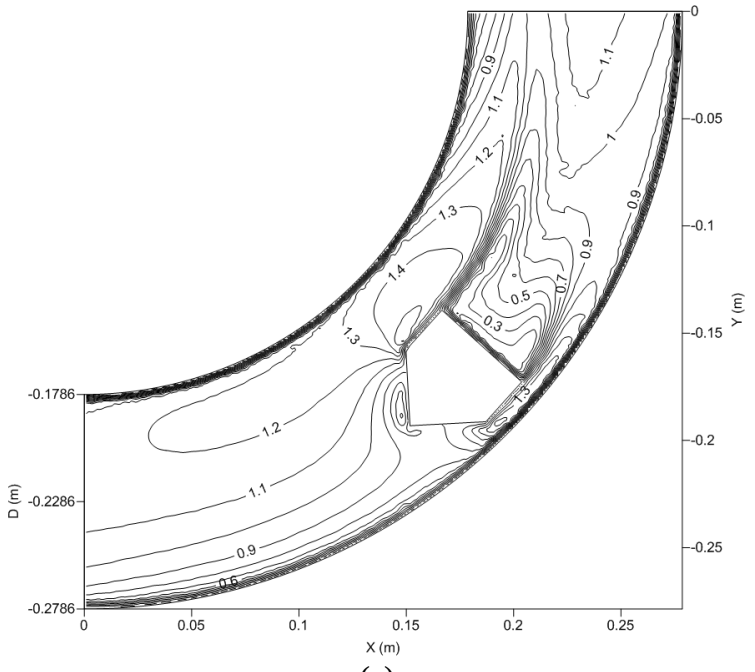
D (m)
X (m)
Y (m)
-0.1786
-0.2286
-0.2786
0
0.05
0.1
0.15
0.2
0.25
-0.05
-0.1
-0.15
-0.2
-0.25

(c)

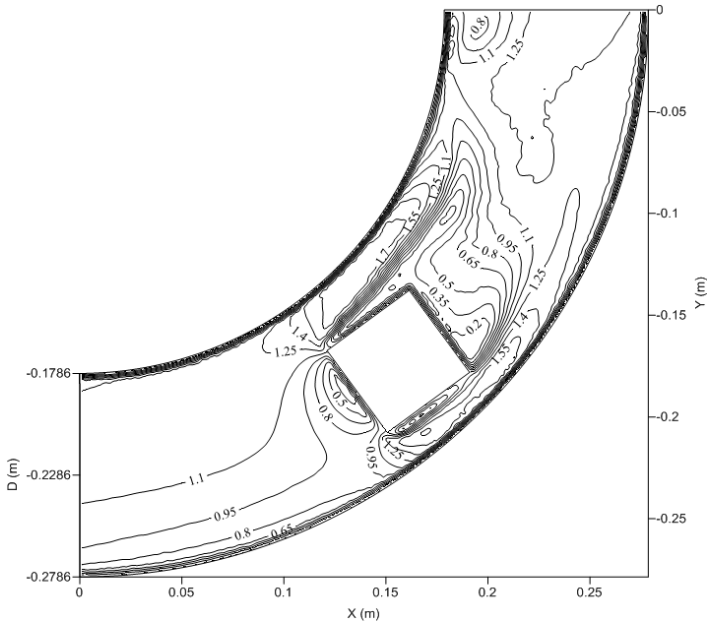

(d)

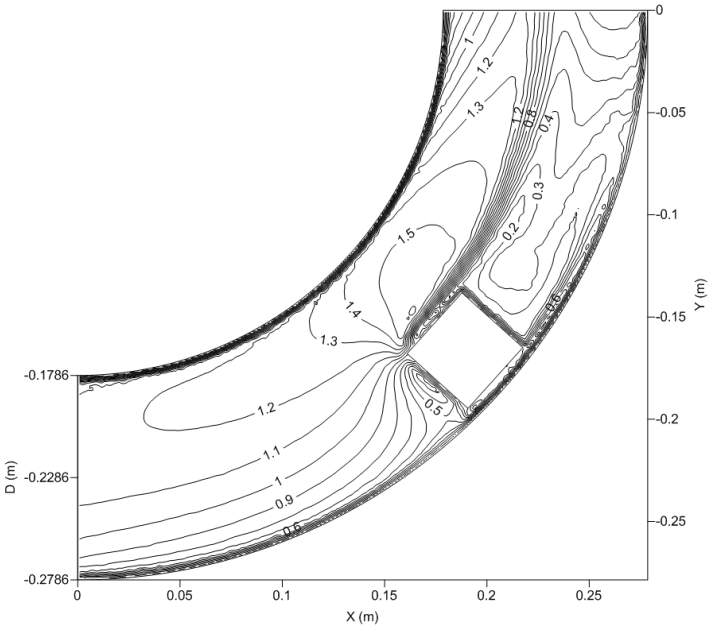

(e)

Figure 11 Flow velocity magnitude variations (in m/sec) within a horizontal HCP bend for the flow of a single equi-density capsule of (a) φ=1 (b) φ=1.004 (c) φ=1.02 (d) φ=2.289 (e) φ=2.481 of k=0.5 at V_{av}=1 m/sec

The effect of capsule motion and its orientation within an HCP has also been investigated. It has been observed that in case of horizontal HCPs, the average pressure drop across the pipeline for different capsule inclinations is within +8% of the results reported here. Similarly, in case of vertical HCPs, the average pressure drop for different capsule inclinations is within +2% of the results presented in this study.

6.0 Effect of capsule density on the flow field within HCPs

Detailed investigations on the flow of heavy-density capsules of different shape factors are important because heavy-density capsules flow differently in horizontal and vertical pipes. As

the specific gravity of the heavy-density capsules is more than 1, in horizontal pipes, these capsules propagate along the bottom wall of the pipe, hence disturbing the axis-symmetric flow distribution. Thus, the distorted velocity profiles in the pipeline leads towards the generation of secondary flows, increasing the losses within the pipeline. In case of heavy-density capsules flowing in vertical pipes however, they still travel along the axis of the pipe, however, due to force balance; the net forward acting force on these capsules is considerably less, resulting in lower capsules' velocities.

Figures 12 and 13 depict the local variations in the pressure coefficient within the test section of both the horizontal and vertical pipes respectively, transporting heavy-density capsules of capsule-to-pipe diameter ratio of 0.5 at an average flow velocity of 1 m/sec. It can be clearly seen in figure 12 that the pressure coefficient variations in the vicinity of the capsules are significantly different to what was observed in case of equi-density capsules. This is due to the positioning of the capsules along the bottom wall of the pipe. However, in case of vertical pipes, in figure 13, the specific gravity of the capsules has no effect on its position. The gap between horizontal pipe's bottom wall and the capsule of φ=2.481 is due to the sharp edges of the capsules which rest on the pipe wall, hence not allowing the bottom face of the capsule to come in contact with the pipe wall.

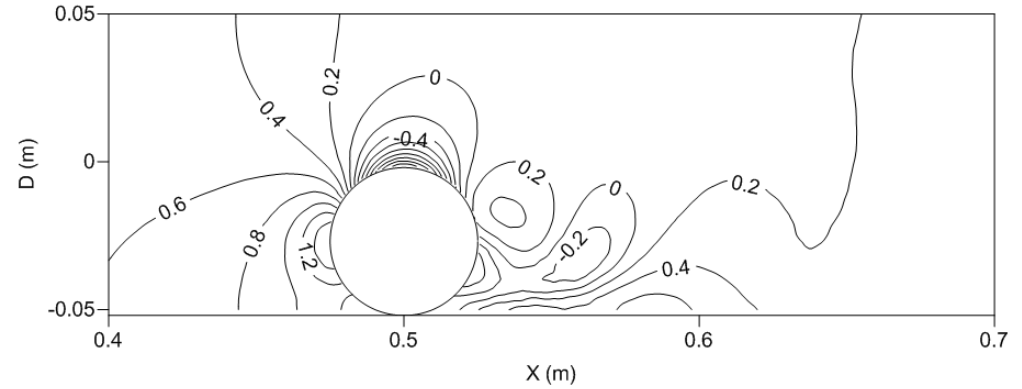

(a)

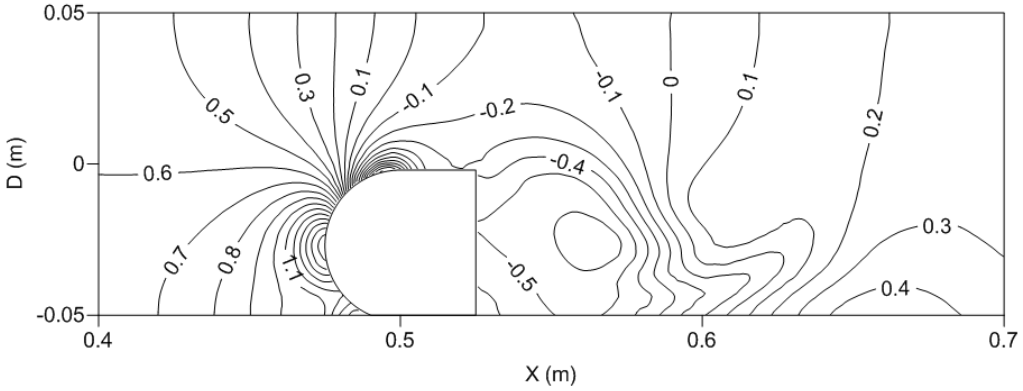

(b)

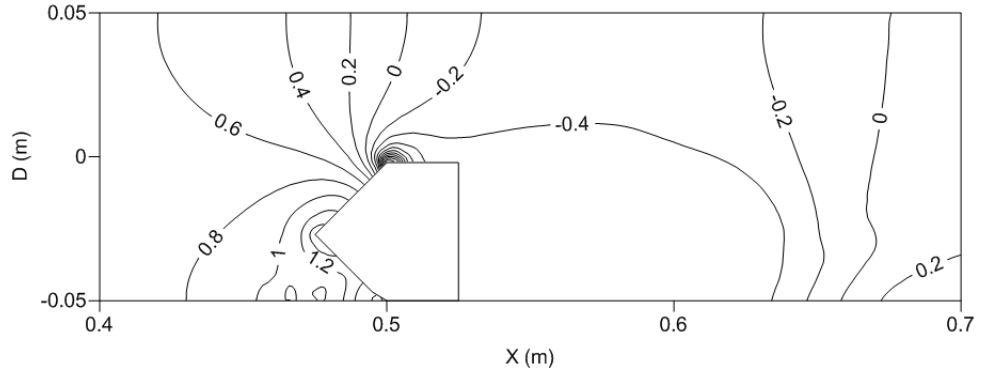

(c)

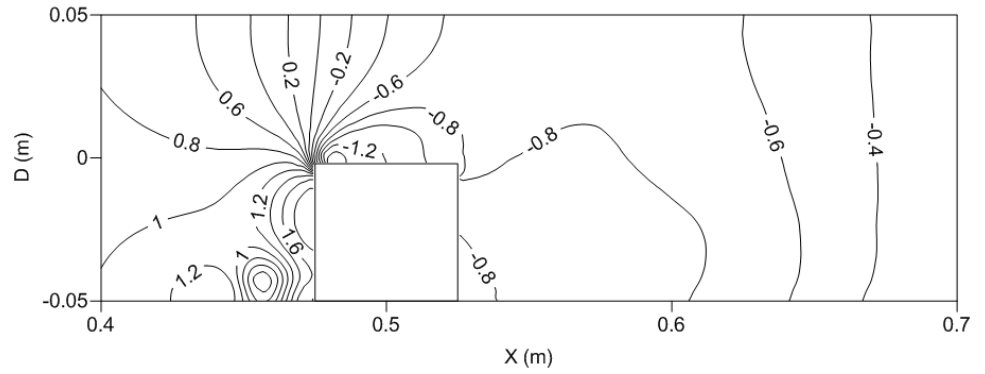

(d)

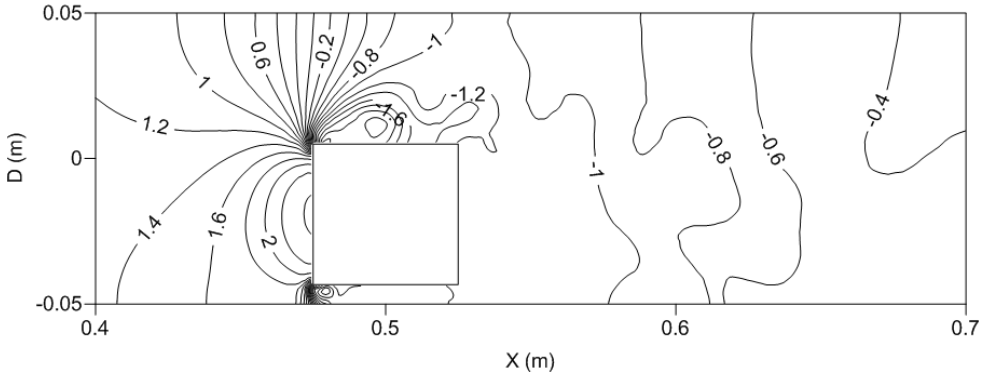

(e)

Figure 12 Pressure coefficient variations within a horizontal HCP for the flow of a single heavy-density capsule of (a) φ=1 (b) φ=1.004 (c) φ=1.02 (d) φ=2.289 (e) φ=2.481 of k=0.5 at V_{av}=1 m/sec

The pressure drops across the horizontal test section for φ=1, 1.004, 1.02, 2.289 and 2.481 are 226 Pa, 236 Pa, 282 Pa, 430 Pa and 472 Pa respectively, which are 35 %, 26 %, 12 %, 26 % and 25 % higher than the equi-density capsules respectively. Similarly, the pressure drops across the vertical test section for φ=1, 1.004, 1.02, 2.289 and 2.481 are 10255 Pa, 10268 Pa, 10333 Pa, 11456 Pa and 11521 Pa respectively. Hence, it can be concluded that as the density of the capsules increases, the pressure drop within the pipeline increases. The results also suggests that the as the shape factor of the capsule increases, the pressure drop across the pipeline increases. Furthermore, it can be concluded that the addition of end shape to the capsules significantly reduces the pressure drop within the pipeline. The increase in the pressure drop within a horizontal HCP carrying heavy-density capsules is due to the positioning of the capsules within the pipeline, while increase in the pressure drop across vertical HCPs carrying heavy-density capsules is due to the relative velocity of the capsules with respect to the carrier fluid.

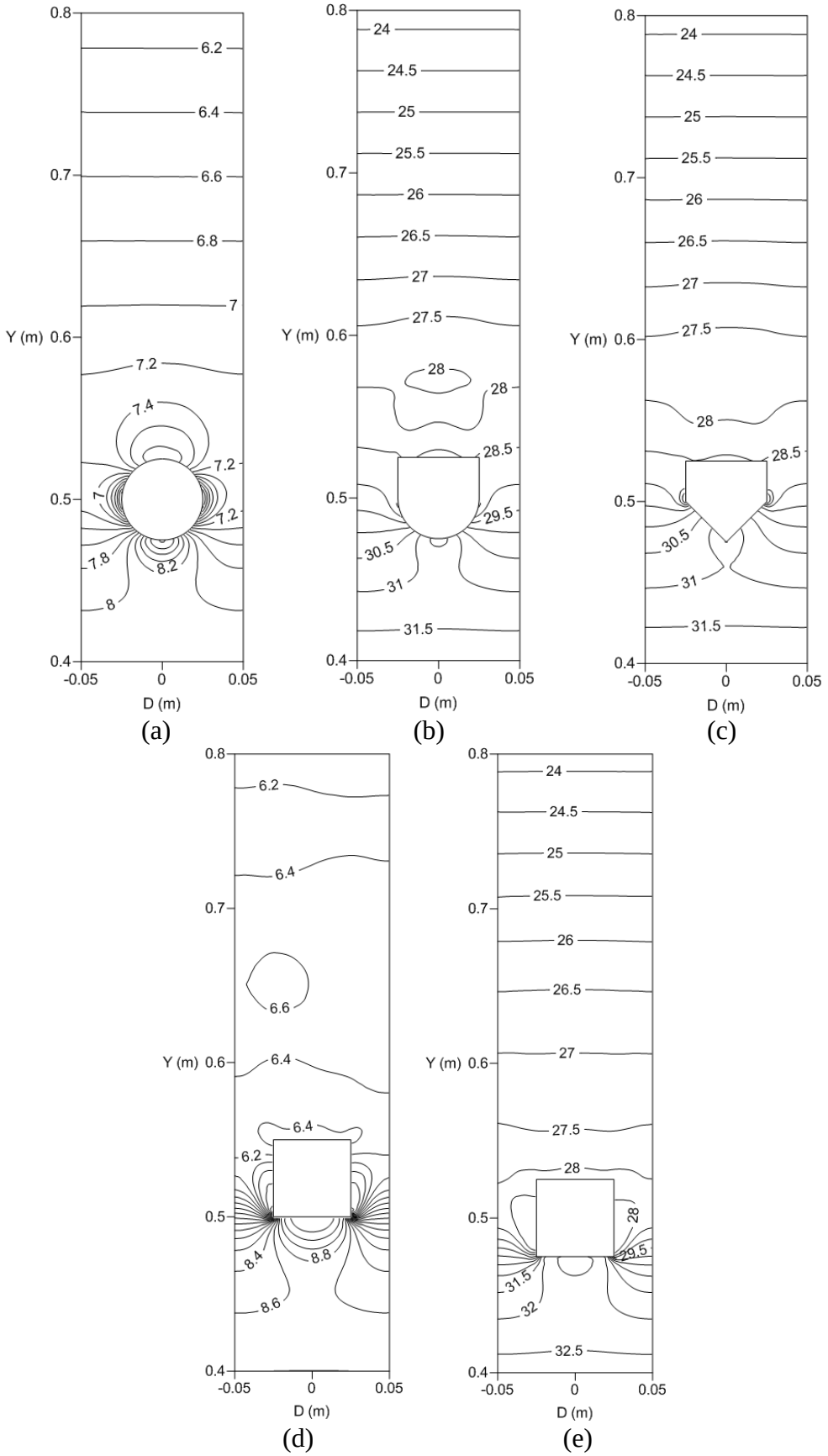

Figure 13 Pressure coefficient variations within a vertical HCP for the flow of a single heavy-density capsule of (a) φ=1 (b) φ=1.004 (c) φ=1.02 (d) φ=2.289 (e) φ=2.481 of k=0.5 at V_{av}=1 m/sec

7.0 Effect of the orientation of capsule on the flow field within HCPs

For a wide range of analysis, the complicated shaped capsules (with end noses) have been considered in the present study to have a different orientation as well, which refers to the end nose located at the downstream end of the capsule/s. Hence, the new shape factors are 1.304 (for hemispherical end) and 1.395 (for conical end). Figures 14 and 15 depict the local variations in the pressure coefficient within the test section of a horizontal pipe, transporting both equi-density (figure 14) and heavy-density (figure 15) capsules. The capsule-to-pipe diameter ratio considered here for analysis is 0.5, while the average flow velocity is 1 m/sec. It can be clearly seen in figures 14 and 15 that the local pressure variations with the test section of the pipeline are significantly different to what has been observed in figures 6 and 12, which corresponds to the end shapes orientated upstream the capsules. The pressure distribution immediately downstream the capsules are more erratic in the case of equi-density capsules. These irregularities in the pressure distribution are expected to cause additional pressure loss within the pipeline, which is discussed later.

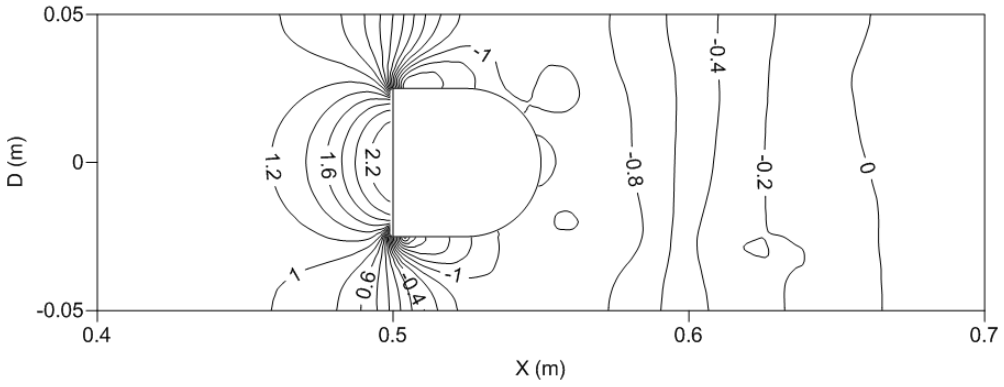

(a)

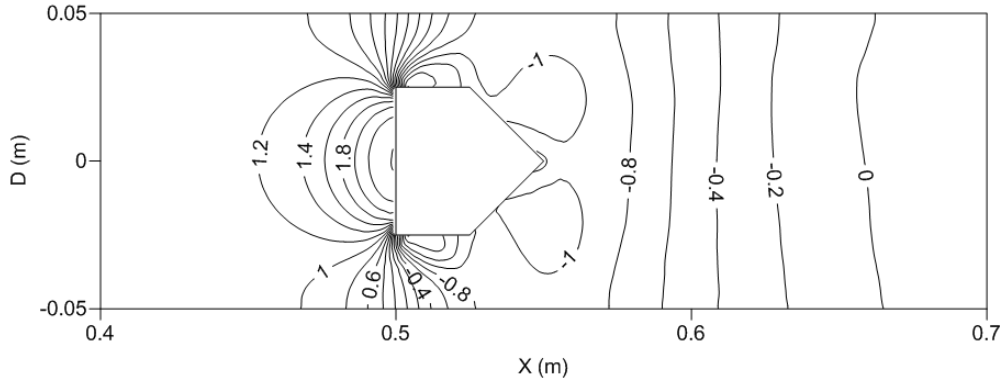

(b)

Figure 14 Pressure coefficient variations within a horizontal HCP for the flow of a single equi-density capsule of (a) φ=1.304 (b) φ=1.395 of k=0.5 at V_{av}=1 m/sec

Comparing figure 15 with figure 12 reveals that when the end shape of the capsule is orientated downstream, the pressure distribution both upstream and downstream the capsule are significantly affected. Especially upstream the capsules, as the flow comes in contact with a flat surface, the pressure distribution resembles the case observed in figure 12(d), which corresponds to a heavy-density capsule of φ=2.289.

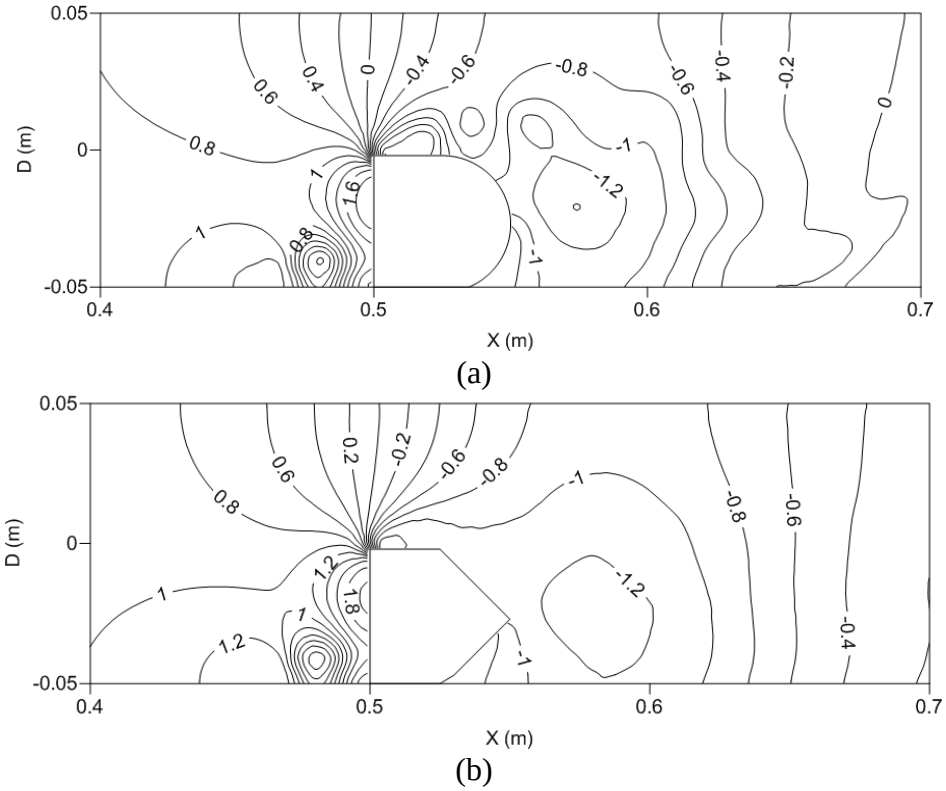

Figure 15 Pressure coefficient variations within a horizontal HCP for the flow of a single heavy-density capsule of (a) φ=1.304 (b) φ=1.395 of k=0.5 at V_{av}=1 m/sec

Further analysing the effects of the location of capsule's end, table 6 summarises the mixture pressure drop being recorded for both equi-density and heavy-density capsules with the corresponding end shapes orientated either ways. It can be clearly seen that when the capsule end shape is orientated downstream the capsule, the pressure drop in the pipeline increases, as compared to the end shapes orientated upstream the capsules. Another important point to note here is that when the end shapes are orientated downstream the heavy-density capsules, the pressure drop across the pipeline is less than for an equi-density capsule with the same shape and orientation of the end nose. Comparing figures 14 and 15 reveal that the secondary flows are generated by the capsule, from either ends, however, in case of heavy-density capsules, only the upper surface of the capsules is exposed to the flow, and hence the secondary flows are observed to generate only from this surface.

Once the pressure drop data has been obtained for a wide range of capsule shape factors and operating conditions, this data has been statistically processed to develop semi-empirical prediction models for capsule's friction factor (in straight pipes) and loss coefficient (in bends). These prediction models have been further embedded into an HCP optimisation model. Table 7 summarises the prediction models developed.

Table 6 Comparison of end shapes of a capsule

End Shape	End Location	φ (-)	s (-)	ΔP_m (Pa)
Hemispherical	Upstream	1.004	1	174
			2.7	236
	Downstream	1.304	1	456
			2.7	376

Conical	Upstream	1.02	1	319
			2.7	430
	Downstream	1.395	1	480
			2.7	471

Table 7 Friction factors and loss coefficients of capsules in HCPs

Pipeline Orientation	Pipe/Bend	f_c and K_{lc} Expressions
Horizontal	Pipe	$f_c = \frac{0.017\,(\varphi+1)^{2.77}\ k^{4.4}\,(s+1)^{0.53}}{\left(\frac{N}{L_p} * L_c\right)^{0.22} Re_c^{\,0.05} \left(\frac{S_c+L_p}{L_p}\right)^{0.71}}$
	Bend	$K_{lc} = \frac{0.33\,(\varphi+1)^{3.58}\,k^{4.4}\,(s+1)^{0.3}}{\left(\frac{N}{L_p} * L_c\right)^{0.38} Re_c^{\,0.01}\ \frac{r}{R}^{0.4} \left(\frac{S_c+L_p}{L_p}\right)^{1.8}}$
Vertical	Pipe	$f_c = \frac{0.01\,(\varphi+1)^{3.93}\,k^{4.5}\ (s+1)^{0.087}}{\left(\frac{N}{L_p} * L_c\right)^{0.27} Re_c^{\,0.015} \left(\frac{S_c+L_p}{L_p}\right)^{0.74}}$
	Bend	$K_{lc} = \frac{5\,(\varphi+1)^{2.16}\,k^{3.57}\,(s+1)^{0.14}}{\left(\frac{N}{L_p} * L_c\right)^{0.24} Re_c^{\,0.097}\ \frac{r}{R}^{0.43} \left(\frac{S_c+L_p}{L_p}\right)^{1.1}}$

In order to verify that these prediction models do match with the CFD predictions of the pressure drop across the pipeline, f_c and K_{lc} from these models have been compared against CFD predicted f_c and K_{lc} values, as shown in figure 16, for both the horizontal and vertical HCPs. It can be clearly seen that more than 90 % of the data points from the developed prediction models lie within ±15 % difference from the CFD predicted f_c and K_{lc} values.

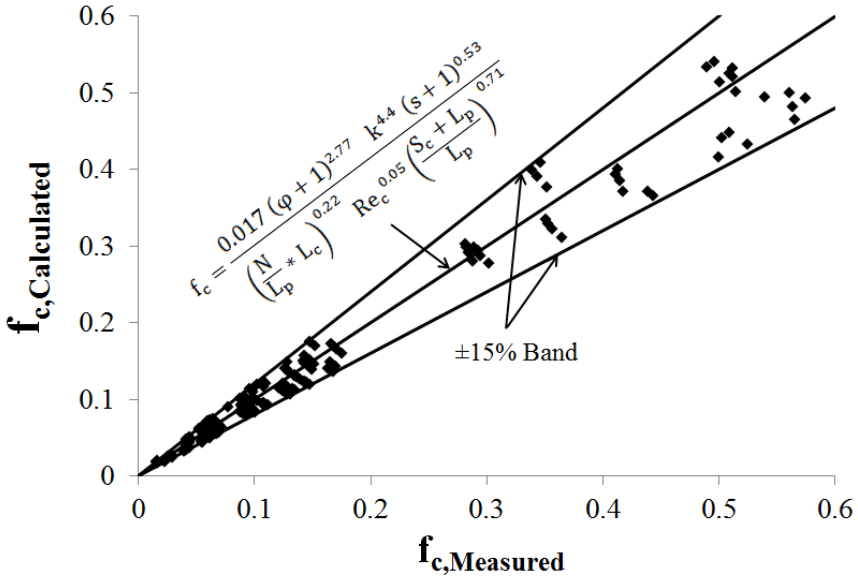
$f_c = \frac{0.017\,(\varphi+1)^{2.77}\ K^{4.4}\,(s+1)^{0.53}}{\left(\frac{N}{L_p} * L_c\right)^{0.22}\ Re_c^{0.05}\left(\frac{S_c+L_p}{L_p}\right)^{0.71}}$
±15% Band
$f_{c,Calculated}$
$f_{c,Measured}$
0
0.1
0.2
0.3
0.4
0.5
0.6

(a)

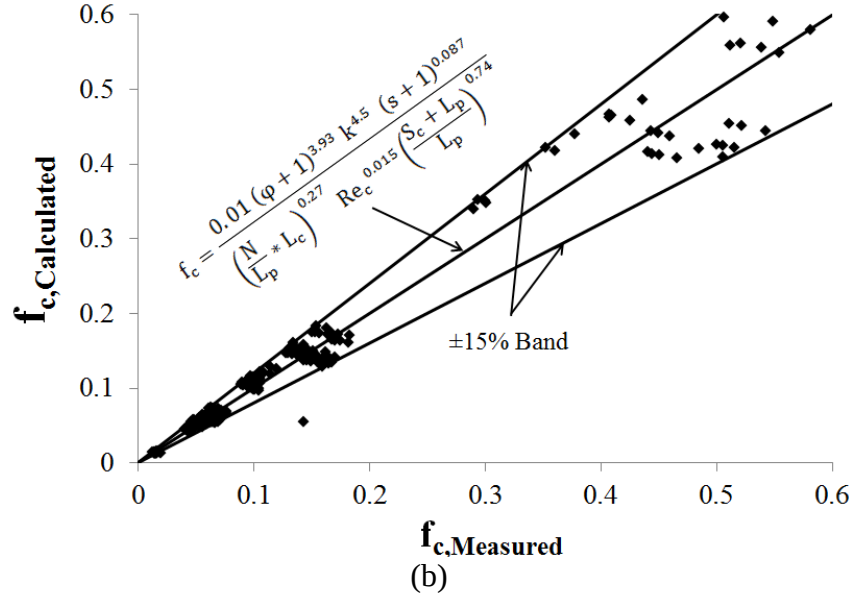
$f_c = \frac{0.01\,(\varphi+1)^{3.93}\ K^{4.5}\,(s+1)^{0.087}}{\left(\frac{N}{L_p} * L_c\right)^{0.27}\ Re_c^{0.015}\left(\frac{S_c+L_p}{L_p}\right)^{0.74}}$
±15% Band
$f_{c,Calculated}$
$f_{c,Measured}$
0
0.1
0.2
0.3
0.4
0.5
0.6

(b)

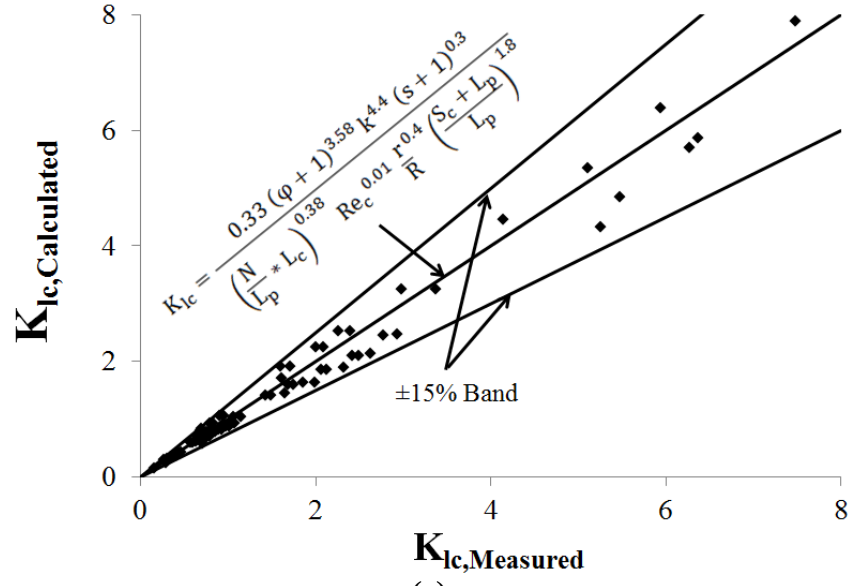
$K_{lc} = \frac{0.33\,(\varphi+1)^{3.58}\ K^{4.4}\,(s+1)^{0.3}}{\left(\frac{N}{L_p} * L_c\right)^{0.38}\ Re_c^{0.01}\ \frac{r^{0.4}}{R}\left(\frac{S_c+L_p}{L_p}\right)^{1.8}}$
±15% Band
$K_{lc,Calculated}$
$K_{lc,Measured}$
0
2
4
6
8

(c)

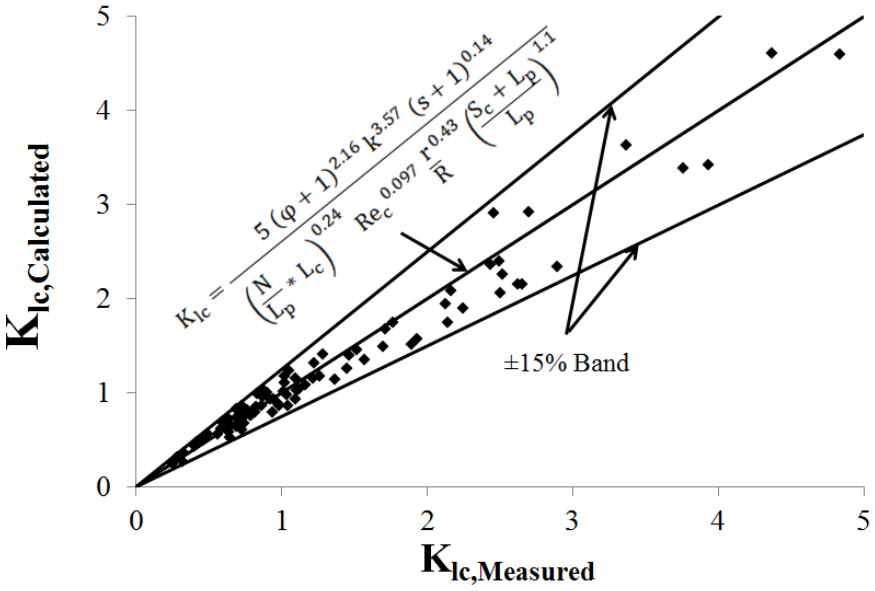

(d)

Figure 16 Comparison between CFD measured and equations based calculated friction factors and loss coefficients for (a) horizontal pipe (b) horizontal bend (c) vertical pipe (d) vertical bend

8.0 Optimisation methodology for hydraulic capsule pipelines

Pipelines designers are always looking towards optimisation to design of pipelines based on different principles, such as least-cost of the pipeline, minimum energy consumption etc. Same is true for hydraulic capsule pipelines as well. In view of this, an optimisation methodology has been developed in the present study for hydraulic capsule pipelines. The developed methodology is based on the least-cost principle; hence, various costs involved in an HCP design have been taken into consideration, and discussed in detail here.

The total cost of an HCP comprises of the manufacturing costs and the operating costs. The manufacturing costs involves the manufacturing of the pipelines itself and the capsules to be transported, while the operating costs constitute the day-to-day operation of the pipeline system, and is also called as the cost of power. Hence:

$$C_{Total} = \left(C_{Pipe} + C_{Capsule}\right) + C_{Power} \tag{12}$$

9.1 Cost of piping material

The cost of pipe per unit weight of the pipe material is given by [58]:

$$C_{Pipe} = \pi D t \Upsilon_p C_2 L_p \tag{13}$$

where t is the thickness of the pipe wall. According to Davis et al [59] and Russel [60], the pipe wall thickness can be expressed as:

$$t = C_c D \tag{14}$$

where C_c is a constant of proportionality dependent on expected pressure and diameter ranges of the pipeline.

9.2 Cost of the capsules

The cost of capsules per unit weight of the capsule material can be calculated as:

$$C_{Capsules} = (SA_c d^2) t_c N \Upsilon_{Cap} C_3 \quad (15)$$

where SA_c is the surface area of the capsules, t_c is the thickness of the capsule wall, N is the number of capsules in the pipeline and Υ_{cap} is the specific weight of the capsule material. The number of capsules in the train/pipeline can be calculated as follows:

$$L_p = NL_c + (N-1)S_c \quad (16)$$

where L_c and L_p are the lengths of the capsule/s and the pipeline, while S_c is the spacing between the capsules. Re-ordering equation (16) gives:

$$N = \frac{L_p + S_c}{L_c + S_c} \quad (17)$$

where L_c is same as d for φ=1 capsules. L_c and S_c should be chosen such that N is an integer.

9.3 Cost of power

The cost of power consumption per unit watt is given by:

$$C_{Power} = C_1 x\, Po \quad (18)$$

where Po is the power requirement of the pipeline transporting capsules. The power controls the selection of the pumping unit for transporting the capsules within the HCP. This power can be expressed as [61]:

$$P = \frac{Q_m \, x \, \Delta P_{Total}}{\eta} \quad (19)$$

where Q_m is the flow rate of the mixture, ΔP_{Total} is the total pressure drop in the pipeline transporting capsules and η is the efficiency of the pumping unit. Liu [62] reports the expression to find the mixture flow rate in a circular pipe as:

$$Q_m = \frac{\pi D^2}{4} V_{av} \quad (20)$$

The total pressure drop can be calculated from equations (3-6), where f_c and K_{lc} have been summarised in table 7, while f_w can be found by the Moody's approximation [63] as:

$$f_w = 0.0055 + \frac{0.55}{Re_w^{\frac{1}{3}}} \quad (21)$$

K_{lw} has been found out to be:

$$K_{lw} = \frac{\left(3.05 - 0.0875\frac{r}{R}\right)}{Re_w^{\frac{1}{5}}} \quad (22)$$

9.4 Solid throughput requirements

Hydraulic capsule pipelines are designed for particular solid throughput requirements; hence the solid throughput (in m^3/sec) is an input to the optimisation model being developed here. The solid throughput can be expressed as:

$$\text{Solid Throughput } (Q_c) = \text{Volume of a capsule x } \frac{\text{Number of capsules in the train}}{\text{Time taken to travel unit length}} \quad (23)$$

The time taken to travel unit distance can be computed as:

$$\text{Time taken to cover 1m distance } = \frac{L_p}{V_c} \quad (24)$$

Combining equations (17, 23-24) gives the solid throughput as:

$$Q_c = Vo_c \text{ x } \frac{L_p+S_c}{L_c+S_c} \text{ x } \frac{V_c}{L_p} \quad (25)$$

where Vo_c is the volume of a capsule. It is important to note here that V_c is calculated using equation (25). Moreover, V_{av} can be represented in terms of V_c from the holdup expressions presented in equations (8-9). The following steps should be followed to run the optimisation model:

1. Assume a value of D. k and d are a function of D, hence automatically calculated.
2. Specify capsule density. s will be automatically calculated.
3. Specify L_c, t_c, C_1, C_2, C_3, C_c, η and the material properties of the pipeline (already known).
4. Specify solid throughput requirements (Q_c).
5. V_c is computed using equation (25) and V_{av} is calculated from equations (8-9). Hence, Re_w and Re_c are automatically calculated.
6. Q_m is computed using equation (20). Q_w is automatically calculated as Q_c is known.
7. Compute the cost of pipe and the capsules.
8. Calculate friction factors and loss coefficients for both water and the capsules. Major, minor and total pressure drops will be automatically computed.
9. Compute the power requirement for the system using equation (19) and the cost of power using equation (18).
10. Calculate the total cost of the pipeline.
11. Repeat steps 1 to 10 for various values of D until that value is reached at which the total cost of the pipeline is minimum.

9.0 HCP design example

The storage area of a processing plant is half a kilometre away. Lead oxide needs to be transferred from the storage area to the plant within capsules of φ=1.004, k=0.5, L_c=3d and t_c of 3 mm, within a steel pipeline. The spacing between the capsules should be 3d. The

required throughput of lime is 0.001 m^3/sec. Find the optimal size of the pipeline and the pumping power (60 % efficient) required for different capsule shapes for this purpose.

Solution: According to the current market, the values of different constants involved in the optimisation process are:

$C_1 = 1.4$ $C_2 = 1.1$ $C_3 = 0.95$ Cc=0.01

Following the aforementioned HCP optimisation steps for the transport of capsules, different costs involved and the required pumping power are summarised in table 8.

Table 8 Variations in pumping power and various costs w.r.t. pipeline diameter for the transport of capsules of φ=1.004

D (m)	$C_{Manufacturing}$ (£)	C_{Power} (£)	C_{Total} (£)	P (kW)
0.04	2531	127102	129633	90.787
0.05	3829	43278	47107	30.913
0.06	5393	17962	23355	12.83
0.07	7223	8546	15769	6.104
0.08	9320	4492	13812	3.209
0.09	11682	2549	14231	1.82
0.1	14311	1535	15846	1.097
0.12	20367	639	21006	0.457
0.14	27487	305	27792	0.218
0.16	35672	161	35833	0.115
0.18	44921	91	45012	0.065

It can be seen in table 8 that as the diameter of the pipeline increases, both the manufacturing and the power costs increases, which in-turn increases the total cost of the pipeline. The increase in the manufacturing cost is because pipes of larger diameters are more expensive as compared to smaller diameter pipes. The increase in the cost of the power is because, for the same solid throughput required, increasing the pipeline diameter decreases the flow velocity within the pipeline, which in-turn decreases the power required from the pumping unit. As the required power decreases, the cost of power also decreases. These trends have been plotted in figure 17, for the costs only. It can be clearly seen that the increase in the manufacturing cost is not directly proportional to the decrease in the cost of power. Hence, the total cost is seen to first decrease upto a certain value of the pipeline diameter, and then it increases. Hence, the effect of the cost of power is dominant on the total cost at lower pipeline diameters, while the manufacturing cost is dominant at larger diameters. Due to this shift in the cost dominance from the manufacturing and power costs, the total cost curve shows a local minima at the point where this shift occurs. The corresponding pipeline diameter is the optimal diameter for the pipeline, for that particular solid throughout required, based on the least-cost principle. It can be seen that that a pipeline of diameter = 8 cm is optimum for the transport of capsules of φ=1.004, k=0.5 and L_c=3d. The corresponding total cost and the required power of the pumping unit are £13,812 and 3.2 kW.

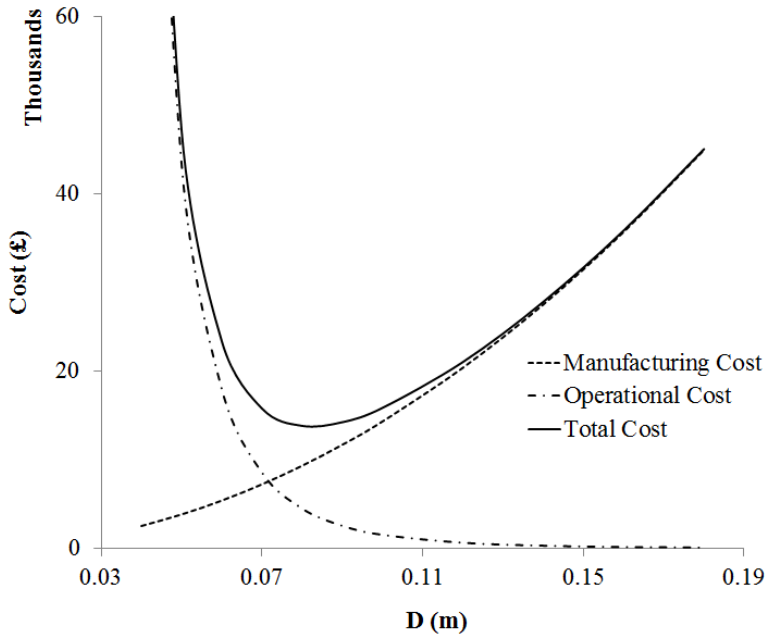

Figure 17 Variations in the different costs of the pipeline w.r.t. pipeline diameter for the transport of capsules of φ=1.004

In order to further analyse the usefulness of the design optimisation methodology developed in the present study, a wide spectrum of the parameters involved is considered. This has led to development of performance charts for HCPs with different shaped capsules (having different shape factors) and different solid throughput requirements. These performance charts are shown in figure 18, where figure 18(a) depicts the variations in the optimal pipeline diameter as a function of the solid throughput and the shape factors of the capsules, while figure 18(b) depicts the variations in the total cost per meter of the pipeline. It can be clearly seen that as the required solid throughput increases, the optimal pipeline diameter and the total cost of the pipeline increases. Moreover, as the shape factor increases, for regular shapes, both the optimal pipeline diameter and the total cost of the pipeline decrease. This is also true for capsules with end shapes; however, the combined trend is non-linear. This means that the capsules with end shapes are more suitable as far as the optimal design of the HCP is concerned. These charts can be used effectively to design an HCP for various operational constraints.

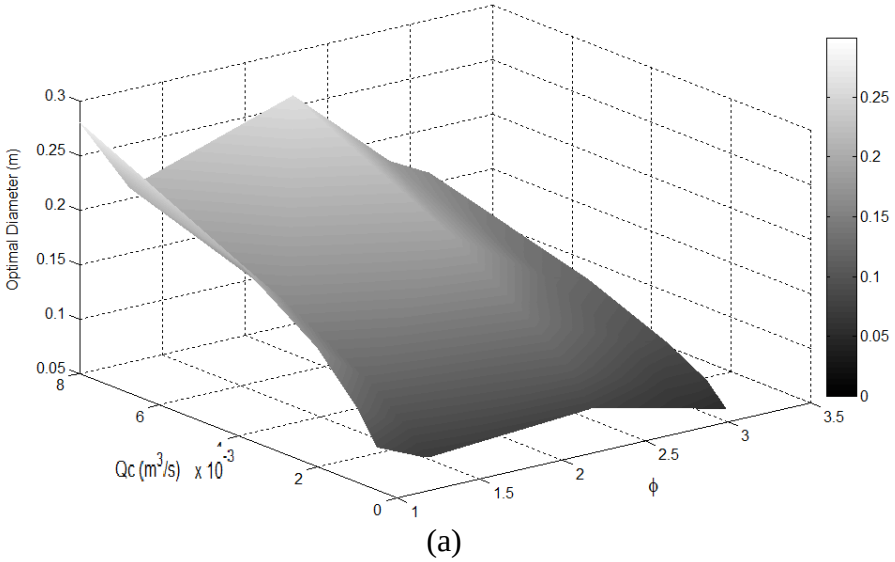

(a)

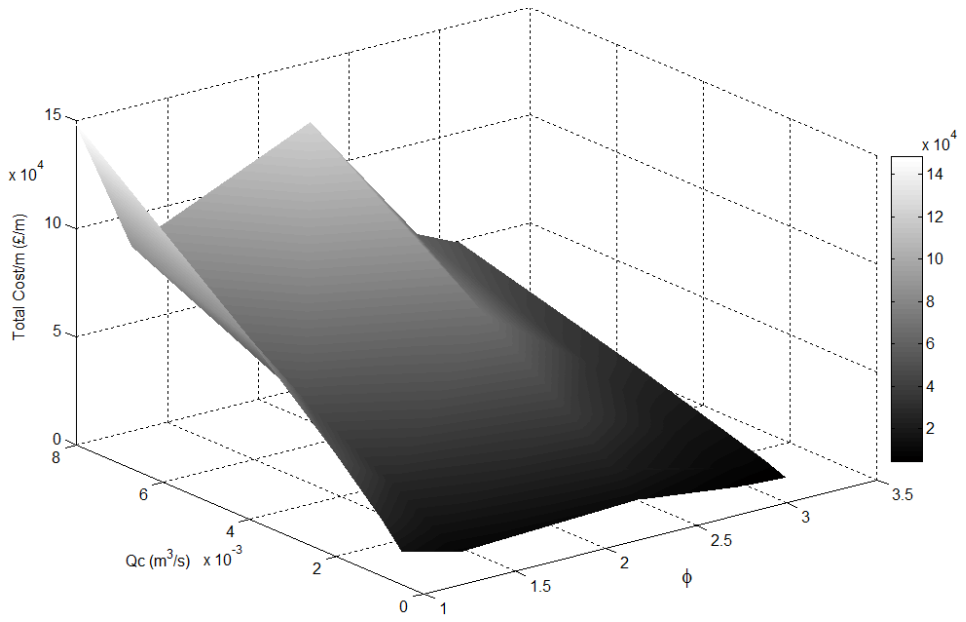

(b)

Figure 18 Effect of the solid throughput required and the shape factor of the capsules on the (a) optimal diameter and (b) total cost per unit length of the pipeline

10.0 Conclusions

The flow of capsules of various shapes have been numerically simulated within hydraulic capsule pipelines for both on-shore and off-shore applications. The effect of the shape factor of the capsules on the pressure distribution within such pipelines has been critically evaluated. Novel semi-empirical pressure drop prediction models have been developed, as a function of the capsules' shape factors, which are then embedded into a pipeline design optimisation model. An example on the usefulness of the optimisation methodology has been presented, with performance charts for a number of practical scenarios being developed.

The results obtained from the numerical simulations indicate that as the shape factor of the capsule increases, the pressure drop across the pipeline also increases. The increase in the shape factor increases pressure non-uniformity within the pipelines. Further pressure non-uniformity has been observed in the case of on-shore hydraulic capsule pipelines, when the density of the capsule/s is higher than that of the carrier fluid. The capsules propagate along the bottom wall of the pipeline, indicating additional energy losses due to contact friction. It has been observed that although the pressure drop across a vertical hydraulic capsule pipeline is considerably higher as compared to a horizontal pipeline, the pressure loss contributions due to presence of the capsules in the flow field remain fairly the same. Moreover, orientating the capsule end shape on its upstream end is recommended, as it causes lower pressure drop across the pipeline. Based on the pressure drop results, novel semi-empirical prediction models have been developed for the friction factors and the loss coefficients of the capsules, as a function of the shape factor of the capsules. These prediction models have been embedded into the pipeline optimisation model. Performance charts for various shaped capsules have been developed in order to aid the designers of hydraulic capsule pipelines.

Nomenclature

c	Concentration of the solid-phase in the mixture (%)
C_c	Constant of proportionality (-)
C_1	Cost of power consumption per unit watt (£/W)
C_2	Cost of pipe per unit weight of pipe material (£/N)
C_3	Cost of capsules per unit wright of capsule's material (£/N)
CSA	Cross-sectional area (m^2)
CG	Centre of gravity (-)
d	Diameter of capsule/s (m)
D	Diameter of pipe (m)
f	Darcy friction factor (-)
g	Gravitational acceleration (m/sec^2)
h	Elevation (m)
H	Holdup (-)
k	Capsule to pipe diameter ratio (-)
K_l	Loss coefficient of bends (-)
L	Length (m)
n	Number of bends (-)
N	Number of capsules (-)
P	Local static pressure (Pa)
Po	Power (W)
Q	Flow rate (m^3/sec)
R	Radius of curvature of pipe bend (m)
r	Radius of the pipe (m)
Re	Reynolds number (-)
s	Specific gravity (-)
SA	Surface area (m^2)
S	Spacing (m)
t	Thickness (m)
V	Velocity (m/sec)
Vo	Volume (m^3)
X	X direction (m)
Y	Y direction (m)

Greek Symbols

ϒ	Specific weight (N/m^3)
Δ	Change (-)
ε	Roughness height of the pipe (m)
η	Efficiency of the pump (%)
μ	Dynamic viscosity (Pa-sec)
л	Pi (-)
ρ	Density (kg/m^3)
ψ or φ	Shape factor (-)

Subscripts

1	Upstream section
2	Downstream section
atm	Atmospheric

av	Average
c	Capsule
m	Mixture
p	Pipe
w	Water

References

[1] Ellis, H. S. (1964) An Experimental Investigation of the Transport by Water of Single Cylindrical and Spherical Capsules with Density Equal to that of the Water, The Canadian Journal of Chemical Engineering, 42, 1 – 8.

[2] Ellis, H. S. (1964) An Experimental Investigation of the Transport by Water of Single Spherical Capsules with Density Greater than that of the Water, The Canadian Journal of Chemical Engineering, 155 – 160.

[3] Ellis, H. S. Kruyer, J. Roehl, A. A. (1975) The Hydrodynamics of Spherical Capsules, The Canadian Journal of Chemical Engineering, 53, 119 – 125.

[4] Ellis, H. S. (1974) Minimising the Pressure Gradients in Capsule Pipelines, The Canadian Journal of Chemical Engineering, 52, 457 – 462.

[5] Ellis, H. S. (1964) An Experimental Investigation of the Transport in Water of Single Cylindrical Capsule with Density Greater than that of the Water, The Canadian Journal of Chemical Engineering, 69 – 76.

[6] Kruyer, J. Redberger, P. J. Ellis, H. S. (1967) The Pipeline Flow of Capsules, Part 9, Journal of Fluid Mechanics, 30, 513 – 531.

[7] Latto, B. Chow, K. W. (1982) Hydrodynamic Transport of Cylindrical Capsules in a Vertical Pipeline, The Canadian Journal of Chemical Engineering, 60, 713 – 722.

[8] Hwang, L. Y. Wood, D. J. Kao, D. T. (1981) Capsule Hoist System for Vertical Transport of Coal and Other Mineral Solids, The Canadian Journal of Chemical Engineering, 59, 317 – 324.

[9] Tachibana, M. (1983) Basic Studies on Hydraulic Capsule Transportation, Part 2, Balance and Start-up of Cylindrical Capsule in Rising Flow of Inclined Pipeline, Bulletin of JSME, 26, 1735 – 1743.

[10] Tsuji, Y. Morikawa, Y. Chono, S. Hasegawa, T. (1984) Fundamental Investigation of the Capsule Transport, 2nd Report, Wake of a Capsule and the Effect of Interaction between Two Capsules on the Drag, Bulletin of JSME, 27, 468 – 474.

[11] Ohashi, A. Yanaida, K. (1986) The Fluid Mechanics of Capsule Pipelines, 1st Report, Analysis of the Required Pressure Drop for Hydraulic and Pneumatic Capsules, Bulletin of JSME, 29, 1719 – 1725.

[12] Bartosik, A. S. Shook, C. A. (1995) Prediction of Vertical Liquid-Solid Pipe Flow Using Measured Concentration Distribution, Particulate Science and Technology, 13, 85 – 104.

[13] Yanaida, K. Tanaka, M. (1997) Drag Coefficient of a Capsule Inside a Vertical Angular Pipe, Powder Technology, 94, 239 – 243.

[14] Chow, K. W. (1979) An Experimental Study of the Hydrodynamic Transport of Spherical and Cylindrical Capsules in a Vertical Pipeline, M. Eng. Thesis, McMaster University, Hamilton, Ontario, Canada.

[15] Mathur, R. Rao, C. R. Agarwal, V. C. (1989) Transport Velocity of Equal Density Spherical Capsules in Pipeline, In the Proceedings of the 4th Asian Congress of Fluid Mechanics, Hongkong, 106 – 109.

[16] Agarwal, V. C. Singh, M. K. Mathur, R. (2001) Empirical Relation for the Effect of the Shape of the Capsules and the End Shape on the Velocity Ratio of Heavy Density

Capsules in a Hydraulic Pipeline, In the Proceedings of the Institute of Mechanical Engineers, Part E: Journal of Process Mechanical Engineering.
[17] Mishra, R. Agarwal, V. C. Mathur, R. (1992) Empirical Relations for Spherical Capsules of Various Densities, In the Proceedings of the 19th National Conference on Fluid Mechanics and Fluid Power, Bombay, India.
[18] Mishra, R. Agarwal, V. C. (1998) Prediction of Holdup in Transport of Spherical Capsules in Pipeline, In the Proceedings of the 3rd International Conference on Fluid Mechanics, Beijing, 681 – 686.
[19] Ulusarslan, D. Teke, I. (2005) An Experimental Investigation of the Capsule Velocity, Concentration Rate and the Spacing between the Capsules for the Spherical Capsule Train Flow in a Horizontal Circular Pipe, Powder Technology, 159, 27 – 34.
[20] Ulusarslan, D. (2010) Effect of Capsule Density and Concentration on Pressure Drops of Spherical Capsule Train Conveyed by Water, Journal of Fluids Engineering, 132.
[21] Ulusarslan, D. (2013) Experimental Investigation of the Effect of Diameter Ratio on Velocity Ratio and Pressure Gradient for the Spherical Capsule Train Flow, European Journal of Mechanics B/Fluids, 37, 42 – 47.
[22] Ulusarslan, D. (2007) Determination of the Loss Coefficient of Elbows in the Flow of Low-Density Spherical Capsule Train, Experimental Thermal and Fluid Science, 32, 415 – 422.
[23] Ulusarslan, D. (2010) Effect of Diameter Ratio on Loss Coefficient of Elbows in the Flow of Low-Density Spherical Capsule Trains, Particulate Science and Technology, 28, 348 – 359.
[24] Ulusarslan, D. Teke, I. (2005) An Experimental Determination of Pressure Drops in the Flow of Low Density Spherical Capsule Train Inside Horizontal Pipes, Experimental Thermal and Fluid Science, 30, 233 – 241.
[25] Uluasarslan, D. (2008) Comparison of Experimental Pressure Gradient and Experimental Relationships for the Low Density Spherical Capsule Train with Slurry Flow Relationships, Powder Technology, 185, 170 – 175 .
[26] Uluasarslan, D. Teke, I. (2008) Comparison of Pressure Gradient Correlations for the Spherical Capsule Train Flow, Particulate Science and Technology, 26, 285 – 295.
[27] Uluasarslan, D. Teke, I. (2009) Relation between the Friction Coefficient and Re Number for Spherical Capsule Train – Water Flow in Horizontal Pipes, Particulate Science and Technology, 27, 488 – 495.
[28] Vlasak, P. and Myska, J. (1983) The Effect of Pipe Curvature on the Flow of Carrier Liquid Capsule Train System, In the Proceedings of the Institute of Hydrodynamics, Praha, Prague.
[29] Vlasak, P. Berman, V. (2001) A Contribution to Hydro-transport of Capsules in Bend and Inclined Pipeline Sections, Handbook of Conveying and Handling of Particulate Solids, 521 – 529.
[30] Kruyer, J. Snyder, W. T. (1975) Relationship between Capsule Pulling Force and Pressure Gradient in a Pipe, The Canadian Journal of Chemical Engineering, 53, 378 – 383.
[31] Charles M. E. (1962) Theoretical Analysis of the Concentric Flow of Cylindrical Forms, The Canadian Journal of Chemical Engineering, 41, 46 – 51.
[32] Kroonenberg, H. H. (1979) A Mathematical Model for Concentric Horizontal Capsule Transport, The Canadian Journal of Chemical Engineering, 57, 383.
[33] Round, G. F. Bolt, L. H. (1965) An Experimental Investigation of the Transport in Oil of Single, Denser-than Oil, Spherical and Cylindrical Capsules, The Canadian Journal of Chemical Engineering, 197 – 205.

[34] Newton, R. Redberger, P. J. Round, G. F. (1963) Numerical Analysis of Some Variables Determining Free Flow, The Canadian Journal of Chemical Engineering, 42, 168 – 173.
[35] Tomita, Y. Yamamoto, M. Funatsu, K. (1986) Motion of a Single Capsule in a Hydraulic Pipeline, Journal of Fluid Mechanics, 171, 495 – 508.
[36] Tomita, Y. Okubo, T. Funatsu, K. Fujiwara, Y. (1989) Unsteady Analysis of Hydraulic Capsule Transport in a Straight Horizontal Pipeline, In the Proceedings of the 6th International Symposium on Freight Pipelines, USA, 273 – 278.
[37] Lenau, C. W. El-Bayya, M. M. (1996) Unsteady Flow in Hydraulic Capsule Pipeline, Journal of Engineering Mechanics, 122, 1168 – 1173.
[38] Khalil, M. F. Kassab, S. Z. Adam, I. G. Samaha, M. A. (2010) Turbulent Flow around a Single Concentric Long Capsule in a Pipe, Applied Mathematical Modelling, 34, 2000 – 2017.
[39] Khalil, M. F. Kassab, S. Z. Adam, I. G. Samaha, M. A. (2009) Prediction of Lift and Drag Coefficients on Stationary Capsule in Pipeline, CFD Letters, 1, 15 – 28.
[40] Polderman, H. G. (1982) Design Rules for Hydraulic Capsule Transport Systems, Journal of Pipelines, 3, 123 – 136.
[41] Assadollahbaik, M. Liu, H. (1986) Optimum Design of Electromagnetic Pump for Capsule Pipelines, Journal of Pipelines, 5, 157 – 169.
[42] Swamee, P. K. (1995) Design of Sediment Transporting Pipeline, Journal of Hydraulic Engineering, 121.
[43] Swamee, P. K. (1999) Capsule Hoist System for Vertical Transport of Minerals, Journal of Transportation Engineering, 560 – 563.
[44] Agarwal, V. C. Mishra, R. (1998) Optimal Design of a Multi-Stage Capsule Handling Multi-Phase Pipeline, International Journal of Pressure Vessels and Piping, 75, 27 – 35.
[45] Colebrook, C.F. (1939) Turbulent Flow in Pipes with Particular Reference to the Transition Region between Smooth and Rough Pipe Laws, Journal of the Institution of Civil Engineers.
[46] Sha, Y. Zhao, X. (2010) Optimisation Design of the Hydraulic Pipeline Based on the Principle of Saving Energy Resources, In the Proceedings of Power and Energy Engineering Conference, Asia-Pacific.
[47] Taimoor Asim (2013) Computational Fluid Dynamics based Diagnostics and Optimal Design of Hydraulic Capsule Pipelines, Ph.D. Thesis, University of Huddersfield, U.K.
[48] Taimoor Asim and Rakesh Mishra (2016) Optimal Design of Hydraulic Capsule Pipeline Transporting Spherical Capsules, The Canadian Journal of Chemical Engineering, 94, 966 – 979.
[49] Taimoor Asim and Rakesh Mishra (2016) Computational Fluid Dynamics based Optimal Design of Hydraulic Capsule Pipelines Transporting Cylindrical Capsules, International Journal of Powder Technology, 295, 180 – 201.
[50] Taimoor Asim, Rakesh Mishra, Sufyan Abushaala and Anuj Jain (2016) Development of a Design Methodology for Hydraulic Pipelines carrying Rectangular Capsules, International Journal of Pressure Vessels and Piping, 146, 111 – 128.
[51] Darcy, H. (1857) Recherches Expérimentales Relatives au Mouvement de l'Eau dans les Tuyaux [Experimental Research on the Movement of Water in Pipes], Mallet-Bachelier, Paris.
[52] Munson, B. R. Young, D. F. Okiishi, T. H. (2002) Fundamentals of Fluid Mechanics, John Willey & Sons Inc., 4th ed., U.S.A., ISBN: 0471675822.
[53] Industrial Accessories Company accessible at http://www.iac-intl.com/parts/PB103001r2.pdf

[54] Mishra, R. Singh, S. N. Seshadri, V. (1998) Improved model for the prediction of pressure drop and velocity field in multi-sized particulate slurry flow through horizontal pipes, Powder Handling and Processing, 10, 279–287.
[55] Mishra, R. Palmer, E. Fieldhouse, J. (2009) An Optimization Study of a Multiple-Row Pin-Vented Brake Disc to Promote Brake Cooling Using Computational Fluid Dynamics, In the Proceedings of the Institution of Mechanical Engineers, Part D: Journal of Automobile Engineering, 223, 865–875.
[56] Mishra, R. Singh, S. N. Seshadri, V. (1998) Velocity measurement in solid-liquid flows using an impact probe, Flow Measurement and Instrumentation, 8, 157–165.
[57] C. Ariyaratne, Design and Optimisation of Swirl Pipes and Transition Geometries for Slurry Transport, Ph.D. Thesis, (2005), The University of Nottingham.
[58] P. N. Cheremisinoff, S. I. Cheng, Civil Engineering Practice, Technomies Publishing Co., U.S.A., 1988.
[59] C. Davis, K. Sorensen, Handbook of Applied Hydraulics, McGraw-Hill Book Co., 3rd ed., U.S.A., 1969.
[60] G. Russel, Hydraulics, Holt, Rinehart and Winston, 5th ed., U.S.A., 1963.
[61] Govier, G. W. Aziz, K. (2008) Flow of Complex Mixtures in Pipes, Society of Petroleum Engineers, 2nd ed., ISBN: 0882755471.
[62] Liu, H. (1992) Hydraulic Behaviours of Coal Log Flow in Pipe, In the Proceedings of the 4th International Conference on Bulk Materials Handling and Transportation; Symposium on Fright Pipelines, Wollongong, Australia.
[63] Moody, L. F. (1944) Friction factors for Pipe Flow, Transactions of the ASME, 66, 671-684.